IPPT PAN
• Institute of Fundamental Technological Research
• Polish Academy of Sciences
• Warsaw • Poland

LECTURE NOTES 15

François Feuillebois

Perturbation Problems at Low Reynolds Number

Centre of Excellence for
Advanced Materials and Structures

WARSAW 2004

AMAS LECTURE NOTES

Production of this volume has been partially supported by the European Commission

Published and distributed by
Institute of Fundamental Technological Research
Świętokrzyska 21, 00-049 Warszawa, Poland

ISSN 1642-0578

Papier offset. kl. III, 70 g, B1
Ark. wyd.: 7,4; ark. druk.: 6,25
Skład w systemie LaTeX: T.G. Zieliński
Oddano do druku i druk ukończono: V 2004
Druk i oprawa: Drukarnia Braci Grodzickich, Piaseczno, ul. Geodetów 47a

Contents

Preface

This series of lectures was given at the Centre of Excellence AMAS in the Institute of Fundamental Technological Research, Polish Academy of Sciences, in October 2003. I am grateful to Prof. Zenon Mróz, scientific coordinator of the AMAS, for his invitation and to various people for making my stay so pleasant and for fruitful discussions; in particular to Dr. Maria Ekiel-Jeżewska, Prof. B. Cichocki, Prof. B.U. Felderhof, Prof. T. Kowalewski. Later interesting discussions with Dr. E. Asmolov are also acknowledged. My special thanks to Dr. Maria Ekiel-Jeżewska and my colleague Dr. Michel Martin for their careful reading of the manuscript.

Notation

Latin letters

Quantities are dimensionless unless otherwise stated. Symbols of dimensional quantities are constructed from dimensionless ones by adding a star superscript (*):

a	:	dimensional sphere radius
$\mathbf{C}$	:	dimensional couple acting on sphere (except in the context of Saffman's equation (3.5))
C	:	$\lvert\mathbf{C}\rvert$
$\mathbf{e}$	:	unit vector
f	:	friction factor
$\mathbf{F}$	:	dimensional force exerted by the fluid on the sphere
F	:	$\lvert\mathbf{F}\rvert$
$\mathbf{F}'$	:	dimensional force exerted by the sphere on the fluid
F'	:	$\lvert\mathbf{F}'\rvert$
h	:	dimensional distance between parallel plane walls
K_1	:	migration velocity coefficient appearing in Eq. (4.4)
K_3^κ	:	migration velocity coefficient appearing in Eq. (4.7)
K_5^κ	:	migration velocity coefficient appearing in Eq. (4.9)
K_3^P	:	migration velocity coefficient appearing in Eq. (4.13)
K_5^P	:	migration velocity coefficient appearing in Eq. (4.3) equivalently, migration velocity coefficient in Eq. (4.13)
l	:	dimensional distance from sphere centre to nearest wall or to a given wall (depending on context)
$\mathbf{n}$	:	unit vector originating from the sphere centre
p	:	perturbed fluid pressure in the frame of the sphere centre
$\overline{p}$	:	perturbed fluid pressure in an absolute frame of reference
P	:	stretched value of p in term of the stretched space variables

$\mathbf{r}$	:	position vector from the sphere centre to a point in the flow field
r	:	$\lvert\mathbf{r}\rvert$
$\mathbf{R}$	:	stretched position vector, Oseen variable
R	:	$\lvert\mathbf{R}\rvert$
$\tilde{\mathbf{R}}$	:	stretched position vector, Saffman variable, defined either from $\sqrt{Re_\kappa}$ or from $\sqrt{Re_p}$, depending on context
$\tilde{R}$	:	$\lvert\tilde{\mathbf{R}}\rvert$
$\mathcal{R}$	:	(1) dimensional tube radius (2) in Saffman's calculation, the radius of a large sphere enclosing fluid
Re	:	Reynolds number based on some relative velocity (in general)
Re_c	:	canal Reynolds number
Re_s	:	Reynolds number based on the slip velocity
Re_κ	:	Reynolds number based on the shear rate κ
Re_p	:	Reynolds number based on the global shear rate U_m/h
t	:	dimensional time
$\mathbf{u}$	:	perturbed fluid velocity in the reference frame of the sphere centre
$\overline{\mathbf{u}}$	:	perturbed fluid velocity in an absolute frame of reference
$\mathbf{U}$	:	value of $\mathbf{u}$ in term of the stretched coordinates
$\mathbf{U}_\infty$	:	dimensional unperturbed fluid velocity
U_m	:	dimensional maximum value of fluid velocity in Poiseuille flow
$\langle U\rangle$	:	dimensional average fluid velocity in Poiseuille flow
$\mathbf{u}_\infty$	:	dimensionless unperturbed fluid velocity
$\mathbf{v}$	:	perturbed fluid velocity in the absolute reference frame (or in the frame of the walls)
$\mathbf{V}$	:	dimensional sphere translational velocity
V	:	$\lvert\mathbf{V}\rvert$
$\mathbf{V}'$	:	$-\mathbf{V}$
V'	:	$\lvert\mathbf{V}'\rvert$
V_m	:	migration velocity of sphere
v_p	:	dimensionless particle translational velocity based on $U_m a/h$
v_r	:	dimensional characteristic velocity of the fluid relative to the particle
V_s	:	slip velocity, viz. velocity of sphere relative to undisturbed flow

V_s' : $-V_s$
x, y, z : coordinates
X, Y, Z : stretched coordinates

Greek letters

ϵ : ratio of the Oseen distance to the Saffman distance
κ : shear rate of shear flow or Poiseuille flow
λ : ratio of the distance to the wall to the Saffman distance
μ : fluid dynamic viscosity
ν : fluid kinematic viscosity
ρ : fluid density
$\boldsymbol{\sigma}$: stress tensor
ξ : $l/h - 1/2$, where l is the distance to a given wall
$\boldsymbol{\Omega}$: dimensional sphere rotational velocity
$\boldsymbol{\omega}$: dimensionless sphere rotational velocity based on V/a
$\boldsymbol{\omega}_p$: dimensionless sphere rotational velocity based on U_m/h

Subscripts

p : denotes dimensionless quantities based on the shear rate U_m/h
S : Stokeslet
SS : Stresslet
x : in the x direction
y : in the y direction
z : in the z direction
0 : in the limit of vanishing Reynolds number (1st term in the expansion for low Reynolds number)
1 : 2nd term in the expansion for low Reynolds number

Superscripts

r : rotational
t : translational
κ : relative to shear flow
* : dimensional

Other symbols

$\tilde{}$: stretched variable or quantity in term of stretched variable, using a Saffman like stretching defined either from $\sqrt{Re_\kappa}$ or from $\sqrt{Re_p}$

$\hat{}$: Fourier transformed

Chapter 1

Introduction

1.1. Motion of particles in the low Reynolds number approximation

The practical goal of this booklet is to show how the motion of small particles in a viscous fluid may be influenced by small fluid inertia effects. The size of particles considered here is typically of the order of 100 μm or smaller and the fluid may be either a liquid or a gas. Such small scales are encountered in various applications, such as separation techniques in analytical chemistry, transport at small scale, microfluidics, biological flow fields, transport of sediments.

The present approach is focusing on the modelling of such microhydrodynamics phenomena, based on the following assumptions:

- Particles considered here are solid in the sense that the fluid velocity should satisfy the classical no-slip boundary condition on their surfaces.
- Moreover, for simplicity, particles are also considered to be spherical. Although this is a somewhat limiting condition, note that small drops in a liquid or in a gas or small bubbles in a liquid may also be considered as solid spherical particles [1] because of impurities adsorbed at their surfaces.
- Suspensions of particles considered here are sufficiently dilute so that the hydrodynamic interactions between particles are negligible. In other words, each particle behaves as if it were alone in the fluid.

- A natural Reynolds number for the flow field around a particle is based on the particle radius, say a, and a characteristic velocity of the fluid relative to the particle, say v_r. This Reynolds number is defined as:

$$Re = \frac{av_r}{\nu}.$$

where ν is the fluid kinematic viscosity. Because of the small size of the particles considered here, this Reynolds number is usually low:

$$Re \ll 1.$$

Note that we write this condition *a priori*; but strictly speaking, the validity of this condition should be verified afterwards, when the fluid velocity has been calculated for the given physical conditions.

The motion of particles in a fluid depends on the force and torque that the fluid exerts on them. In order to obtain these main quantities, the flow field around each particle has to be determined first. The Navier-Stokes equations for the flow around a particle are written in dimensionless form as:

$$\nabla \cdot \overline{\mathbf{u}} = 0, \tag{1.1a}$$

$$\underline{Re\left(\frac{\partial \overline{\mathbf{u}}}{\partial t} + \overline{\mathbf{u}} \cdot \nabla \overline{\mathbf{u}}\right)} = -\nabla \overline{p} + \nabla^2 \overline{\mathbf{u}}, \tag{1.1b}$$

where $\overline{\mathbf{u}}, \overline{p}$ are the "perturbed" fluid velocity and pressure (viz. perturbed by the presence of the particle). From the assumption of a low Reynolds number $Re \ll 1$, the underlined inertial terms drop out and we obtain Stokes equations which are linear. As shown in detail in Sec. 1.2, the linearity of Stokes equations implies that the velocity of a particle is usually aligned with that of the ambient or "unperturbed" fluid flow. As a result, particles follow the streamlines of that flow.

However, a cornerstone experiment by Segré & Silberberg (presented below in Sec. 1.3) showed that small particles in a pipe flow migrate across streamlines. This unexpected result, apart from being a curiosity, has now various applications; for example, it is now currently used in separation techniques presented in Sec. 1.4. As to the reason for the particles migration, Segré & Silberberg anticipated that it is due to fluid inertia effects. That is, the modelling should consider a non-zero Reynolds number. The Reynolds number being small, a second order expansion in Re has to be derived. But performing a second order expansion in Re may raise a singular perturbation problem (in the sense defined e.g. in the handbook of van Dyke [2]). Some background about singular perturbation problems related to small fluid inertia effects will be given in Sec. 1.5. It will be shown why some perturbation problems happen to be singular while others involve simply a regular perturbation, that is a straightforward expansion for low Reynolds number.

The quest for the modelling of Segré & Silberberg experiment was an incentive for many theoretical papers solving various perturbation problems for low Reynolds number. These works, briefly presented in Sec. 1.6, are considered in detail in the following Chapters. Some perturbation problems are singular and some others regular. Both types of problems will be presented.

Before going into these theories, we start by some background about the Stokes equations.

1.2. Properties of the Stokes equations. The Bretherton argument

When $Re \to 0$ the Navier-Stokes equations (1.1) reduce to the Stokes equations:

$$\boldsymbol{\nabla} \cdot \overline{\mathbf{u}} = 0, \tag{1.2a}$$

$$\boldsymbol{\nabla} \overline{p} = \nabla^2 \overline{\mathbf{u}}. \tag{1.2b}$$

Since the original work of Stokes [3], there has been numerous solutions of the Stokes equations for the flow around particles (see e.g. [4]). An interesting consequence of the linearity of these equations was pointed out by Bretherton [5].

Consider e.g. a spherical particle held fixed in a shear flow (far from the particle) along a wall (see Fig. 1.1). This particle is submitted to a force which may a priori have any direction; that is, the force represented in Fig. 1.1(left)

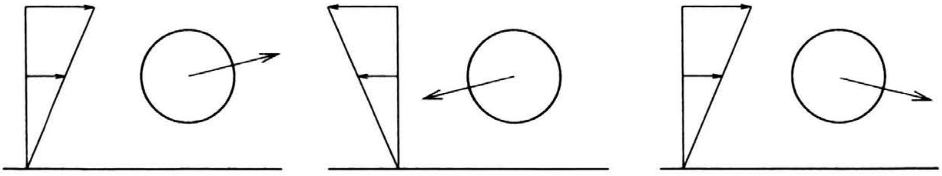

FIGURE 1.1. Application of Bretherton argument.

has a drag component in the same direction as the incident shear flow and a lift component perpendicular to it. Now reverse time. From linearity of Stokes equations, if the shear flow velocity is reversed, so are the local fluid velocity around the particle and the local pressure perturbation (relative to the pressure at infinity). From the linearity of the integral of stresses on the particle, the force exerted by the fluid is reversed as shown in Fig. 1.1(middle). Next, transform the figure with a symmetry relative to a plane perpendicular to the wall and to the velocity at infinity. Obviously (Fig. 1.1, right), the original shear flow at infinity is recovered, whereas the force on the sphere is not. But having a different flow field is impossible by uniqueness of the solution of the Stokes equations. The only possibility for the force to be unchanged is that *the lift component vanishes.*

This argument may be repeated to show that a freely moving sphere in the same condition will move along the wall.

Note that the problem of a freely moving sphere in a shear flow along a wall may be obtained, again from linearity of the Stokes equations, by adding up several flow fields:

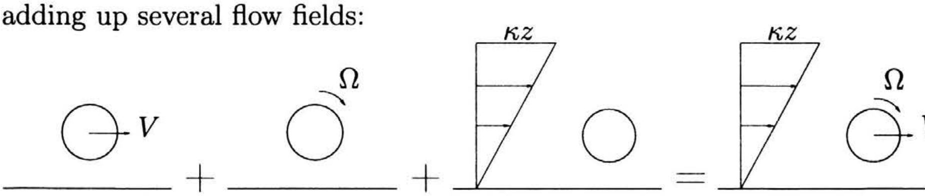

$$
\begin{array}{ccccccccc}
-6\pi a\mu f^{t}_{xx}V & + & 6\pi a^2\mu f^{r}_{xy}\Omega & + & 6\pi a\mu f^{\kappa}_{xx}\kappa l & = & F^* & = & 0, \\
8\pi a^2\mu c^{t}_{yx}V & - & 8\pi a^3\mu\, c^{r}_{yy}\Omega & + & 4\pi a^3\mu c^{\kappa}_{yx}\kappa & = & C^* & = & 0.
\end{array}
$$

As shown schematically, adding up flow fields due to a sphere translating (with velocity V) and rotating (with velocity Ω) in a fluid at rest and that due to a sphere held fixed in a shear flow (κz, where z is the coordinate normal to the wall) gives the problem of a sphere translating and rotating in a shear flow. Each of the first three flow fields gives a force and a torque on the sphere, which by linearity of the Stokes equation are respectively proportional to the relevant characteristic velocities. Here the forces and torques are normalized (μ denotes the dynamic viscosity) and we defined dimensionless friction coefficients denoted with f for the forces and c for the torques. For the translation problem, the motion along the wall (say, along x) gives a force along x and the friction coefficient is denoted f^t_{xx}. When the sphere is far away from the wall, the classical Stokes [3] drag force should be recovered so that $f^t_{xx} \to 1$; this is the reason for the present normalization. Likewise for the rotation problem along axis y (perpendicular to the plane of the figure), there is a torque along y with normalized friction coefficient c^r_{yy}. When the sphere is far away from the wall, the classical rotation problem for a sphere in infinite fluid is recovered provided $c^r_{yy} \to 1$. The normalization for the shear flow problem comes from Faxen relation in infinite fluid (see e.g. [4]). Here, l denotes the distance from the sphere centre to the wall. From the linearity of the expressions for the force and torque, the values F^*, C^* for the final problem are then obtained by summing up the ones for the three composing problems. Now, if the sphere is freely moving, both F^* and C^* vanish. This gives a linear system to be solved for the translational velocity V and rotational velocity Ω. The solution is then:

$$V = \frac{f^\kappa_{xx} c^r_{yy} + f^r_{xy} c^\kappa_{yx} \frac{a}{2l}}{f^t_{xx} c^r_{yy} - f^r_{xy} c^t_{yx}} \kappa l, \qquad \Omega = \frac{f^t_{xx} c^\kappa_{yx} + f^\kappa_{xx} c^t_{yx} \frac{2l}{a}}{f^t_{xx} c^r_{yy} - f^r_{xy} c^t_{yx}} \frac{\kappa}{2}.$$

This approach is classical [6, 7]. Novel more precise results for these problems have been obtained by the method of bipolar coordinates [8]. In any case, there is no lift on the sphere and no migration velocity (that is no velocity perpendicular to the flow at infinity) as anticipated from Bretherton argument.

That is, whenever experimental results show that a spherical particle is submitted to a lift force or a migration velocity, this is due to non-linear inertial terms of the Navier-Stokes equations; then a second order expansion in *Re* is needed to model it. Such lift forces or migration velocities were for the first time described in detail in the Segré & Silberberg experiment, that we will present now.

1.3. The Segré & Silberberg experiment

In this experiment [9] (cf. also the more comprehensive reports in [10, 11]), neutrally buoyant spherical particles are injected in a Poiseuille flow in a tube. The data are as follows:

Tube radius	$\mathcal{R} = 1.16\,\mathrm{cm}$
Mean velocity	$\langle U \rangle \simeq 0.5\,\mathrm{m/s}$
Fluid viscosity	$\mu = 0.4\,\mathrm{Pa.s}$
Fluid density	$\rho = 1.18\,\mathrm{g/cm^3}$
Pipe Reynolds number	$2\mathcal{R}\,\langle U \rangle \rho/\mu = 17$
Particles density	= fluid density
Particles diameter	$2a = 0.8$ to $1.6\,\mathrm{mm}$

Particles are uniformly distributed at the tube entrance and it is observed that at some distance downstream the particles gather at mid-distance between the tube centre and the wall, as shown schematically in Fig. 1.2. This appears as a "tubular pinch" [9]. The final distribution sketched in Fig. 1.2 only appears after a distance from the tube entrance $\ell \sim 1/\langle U \rangle$, thus after an advection time $t \sim \ell/\langle U \rangle \sim 1/\langle U \rangle^2$ giving a radial velocity $\sim \mathcal{R}/t \sim \langle U \rangle^2$. Since this radial velocity is proportional to the square of the mean velocity in the tube, Segré & Silberberg claimed that the migration of particles across streamlines is due to fluid inertia. The following theories prove that they were right.

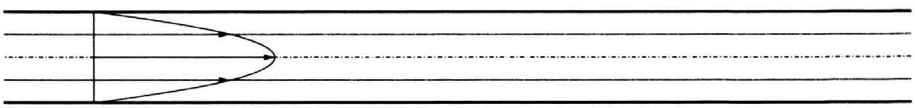

FIGURE 1.2. Schematic representation of the final equilibrium position of neutrally buoyant particles in Poiseuille flow [9], at mid-distance between the tube axis and the tube wall.

In the aerodynamic literature, it is known that a combination of translation and rotation in the motion of fluid at high Reynolds number around a body gives a lift force; this is the so-called Magnus effect [1)]. Then, Segré & Silberberg anticipated some kind of Magnus effect which, as the following theories will show, is not right but not far from the truth.

They also realized that a lift force would make particles migrate across the streamlines without stopping, so that some wall effects were needed to explain the peculiar distance to the wall; following theories prove that they were also right.

1) The lift force on a sphere is sometimes also called the Robins effect, the Magnus effect then being then the lift force on a cylinder, see e.g. [12].

Finally, they anticipated that "it may find application in the fractionation of particles of different sizes", which is realized today by the *Field Flow Fractionation (FFF)* technique in analytical chemistry.

The articles [9, 10, 11] were followed by other experiments designed to observe the migration of spheres in circular tubes (see e.g. the review in [13]).

1.4. Separation techniques in analytical chemistry

Two techniques will be briefly presented here. For a more comprehensive review, the reader could consult e.g.[14].

The *Field Flow Fractionation (FFF)* consists essentially of a Poiseuille flow between two close walls: the distance between walls is a fraction of a millimeter and the length of the canal is of the order of 50 cm. The canal being horizontal, particles are first injected at the canal entrance. As opposed to the Segré & Silberberg experiment in which the particles were neutrally buoyant, particles to be separated are usually heavy and therefore settle down towards the lower wall. Then the flow is started. For non-Brownian suspensions (the particle size being typically larger than a micrometer), it is observed that the largest particles arrive first at the end of the canal, as represented schematically in Fig. 1.3. This is because the large particles migrate higher than the smaller ones and then reach streamlines with a higher velocity. This is called the "hyper-layer" mode in FFF (as opposed to the "classical" mode for which the larger the particle, the lower the streamline as intuitively expected; that mode occurs for Brownian suspensions). Indeed, Segré & Silberberg found that the migration velocity varies like a^4. Such a migration velocity also occurs here and is due to a lift force varying like a^4. Particles eventually reach an equilibrium position in which the lift force balances the weight (which varies like a^3), so that a separation in sizes occurs.

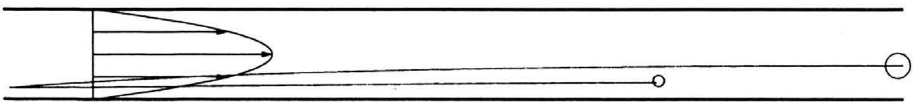

FIGURE 1.3. Schematic representation of the migration of particles in Field Flow Fractionation in the "hyperlayer" mode. Particles with a larger diameter migrate higher and thus move faster along the tube so that they are separated from smaller particles.

In the *SPLIT Thin flow fractionation (SPLITT) cell*, the canal is similar to the one in FFF but is separated typically in two parts at the entrance and at the exit, as represented schematically in Fig. 1.4. A mixture of different particles is injected in the upper part of the entrance. Some heavier particles settling down faster come out through the lower exit whereas lighter particles come out through the upper one. As opposed to FFF, this is a continuous separation process. In general, particles to be separated are moved across streamlines by some field force (not necessarily gravity). Also, the relative flow rates in the two entrance and two exit channels may be adjusted, which is practically equivalent to adjustable separations.

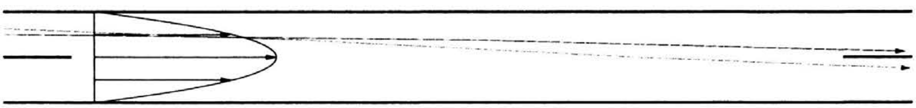

FIGURE 1.4. Schematic representation of the SPLIT Thin flow fractionation, or "SPLITT" cell. In a force field, say gravity, heavier particles move down faster and are separated in the lower exit whereas lighter particles leave through the upper exit.

In the present case, the migration velocity due to the shear rate is not large enough to lift particles like in FFF. However, it is still present and appears as a hindrance which must be taken into account.

1.5. Small fluid inertia effects for a translating sphere. Whitehead paradox and Oseen solution

Before entering into the details of various theories, some background on the second order perturbation solutions for low Reynolds number is presented. It is important to distinguish between *regular* and *singular* perturbation problems and the conditions for which these different cases arise will now be exposed.

We start with the classical Whitehead paradox which appeared in the course of the calculation of a second order term following the classical Stokes result.

1.5.1. Whitehead paradox

Consider a sphere moving with velocity $\mathbf{V}$ in a fluid at rest. For vanishing Reynolds number $Re = Va/\nu$ (where $V = |\mathbf{V}|$), the Navier-Stokes equations (1.1) give the Stokes equations (1.2) as seen above. The solution of these equations for this translation problem was obtained by Stokes himself [3]. The results for the fluid velocity and pressure are in a fixed frame of reference:

$$\overline{\mathbf{u}}^* = \frac{3a}{4}\frac{[\mathbf{V}+\mathbf{n}(\mathbf{V}\cdot\mathbf{n})]}{r^*} + \frac{a^3}{4}\frac{[\mathbf{V}-3\mathbf{n}(\mathbf{V}\cdot\mathbf{n})]}{r^{*3}}, \tag{1.3a}$$

$$\overline{p}^* = \frac{3a}{2}\mu\frac{(\mathbf{V}\cdot\mathbf{n})}{r^{*2}}. \tag{1.3b}$$

Here and below, quantities with a star superscript (*) are dimensional (quantities without the star will be non-dimensional, except the sphere velocity that will always be denoted $\mathbf{V}$ for simplicity). Let $\mathbf{r}^*$ denote a position vector from the sphere centre to a point in the flow field, $r^* = |\mathbf{r}^*|$ and $\mathbf{n} = \mathbf{r}^*/r^*$ a unit vector. Integrating the stress ($\boldsymbol{\sigma}^* \cdot \mathbf{n}$, where $\boldsymbol{\sigma}^*$ is the stress tensor) due to this flow field on the sphere surface, Stokes found the now celebrated expression for the drag on the sphere:

$$\mathbf{F}^* = -6\pi a\mu\mathbf{V}.$$

It is important for the following developments to calculate the flow field obtained by a point force applied to the fluid, or *Stokeslet*. This flow is obtained when the sphere becomes vanishingly small, that is $a \to 0$, at constant $\mathbf{F}'^* = -\mathbf{F}^*$, where $\mathbf{F}'^*$ is the force acting on the fluid. The result for the velocity is the first term, that is the one in $1/r^*$ in (1.3a):

$$\mathbf{v}_S^* = \frac{\mathbf{I}+\mathbf{nn}}{r^*}\cdot\left(\frac{\mathbf{F}'^*}{8\pi\mu}\right)$$

where $\mathbf{I}$ is the identity tensor. Note that the second term in (1.3a) then amounts to a volume effect of the sphere. The result for the pressure due to a point force is simply from (1.3b):

$$p_S^* = \frac{\mathbf{F}'^*\cdot\mathbf{n}}{4\pi r^{*2}}.$$

We now proceed to calculate the second order term in $Re \ll 1$. We use a frame moving with the sphere centre in which the flow field is steady. The fluid velocity in this frame is $\mathbf{u}^* = \overline{\mathbf{u}}^* - \mathbf{V}$ and the velocity at infinity is $\mathbf{V}' = -\mathbf{V}$. Dimensionless quantities are defined with a as a reference length and $\mathbf{V}'$ as a reference velocity. Thus, the dimensionless fluid velocity $\mathbf{u}$ satisfies $\mathbf{u} \to \mathbf{e}_x$ at infinity, where $\mathbf{e}_x$ denotes a fixed unit vector. The other boundary condition is $\mathbf{u} = 0$ on the sphere.

The non-dimensional Navier-Stokes equations for the flow around the sphere are:

$$\boldsymbol{\nabla} \cdot \mathbf{u} = 0, \tag{1.4a}$$

$$\underline{Re\,(\mathbf{u} \cdot \boldsymbol{\nabla}\mathbf{u})} = -\boldsymbol{\nabla} p + \nabla^2 \mathbf{u}. \tag{1.4b}$$

The unknown fluid velocity and pressure are searched as expansions:

$$\begin{aligned} \mathbf{u} &= \mathbf{u}_0 + Re\,\mathbf{u}_1, \\ p &= p_0 + Re\,p_1. \end{aligned}$$

Introducing these expansions into the Navier-Stokes equations (1.4), we obtain Stokes equations for $(\mathbf{u}_0, p_0)$, the solution of which is given in dimensional form in (1.3); and for $(\mathbf{u}_1, p_1)$:

$$\boldsymbol{\nabla} \cdot \mathbf{u}_1 = 0, \tag{1.5a}$$

$$-\boldsymbol{\nabla} p_1 + \nabla^2 \mathbf{u}_1 = \mathbf{u}_0 \cdot \boldsymbol{\nabla} \mathbf{u}_0, \tag{1.5b}$$

with boundary conditions: $\mathbf{u}_1 = 0$ on the sphere, $\mathbf{u}_1 \to 0$ at infinity. Proceeding to solve this problem, Whitehead [15] found that the boundary condition at infinity cannot be applied. It is realized today that this is a singular perturbation problem at infinity but at that time it appeared as a paradox.

1.5.2. Oseen scaling

Indeed, as observed by Oseen [16], in the Navier-Stokes equations (1.4) the underlined inertial term $Re\,(\mathbf{u} \cdot \boldsymbol{\nabla}\mathbf{u})$ is of the same order as the viscous term $\nabla^2\mathbf{u}$ at a normalized distance $\ell \sim 1/Re$. Then the straightforward expansion breaks down. In order to describe the flow field at distances of the order of ℓ, it is then appropriate to stretch the space variable $\mathbf{r}$ by using an Oseen variable:

$$\mathbf{R} = Re\,\mathbf{r}.$$

If we keep $|\mathbf{R}|$ of the order of unity in the process $Re \to 0$, then $|\mathbf{r}|$ is of the order of $1/Re$. This is the Oseen limit process, which applied to Navier-Stokes equations then gives Oseen equations. That is, Oseen equations are valid at such large distances $Ord(1/Re)$ whereas the second order Stokes equations which Whitehead tried to solve are only valid near the sphere.

The adequate technique to reconcile these descriptions was later formalized by the pioneer work of Kaplun [17]. Classical notions about singular perturbation problems and their treatment by the method of matched asymptotic expansions are recalled in Appendix A. For a more thorough presentation, the reader could consult e.g. [2].

As to the Oseen problem, the proper way to proceed further will be described in Chapter 2 which will cover the more general problem of a translating and rotating sphere.

1.5.3. Saffman scaling

The Oseen variable is appropriate to the translational problem, but in general the suitable stretched coordinate depends on the flow at infinity. Saffman [18] considered a sphere moving in an undisturbed shear flow (i.e. a shear flow at large distance from the sphere) with shear rate κ. Then the Reynolds number based on the shear rate is defined as:

$$Re_\kappa = \kappa a^2/\nu.$$

It is assumed to be low compared with unity. Again, the second order problem in Re_κ is singular at infinity. The inertial term in the Navier-Stokes momentum equation then scales as: $Re_\kappa\,(\mathbf{u}\cdot\nabla\mathbf{u}) \sim Re_\kappa\,(\ell\,\nabla\mathbf{u})$. It is of the order of the viscous term $\nabla^2\mathbf{u}$ at a normalized distance $\ell \sim 1/\sqrt{Re_\kappa}$. Then the appropriate stretched variable is Saffman variable:

$$\tilde{\mathbf{R}} = \sqrt{Re_\kappa}\,\mathbf{r}.$$

1.5.4. Regular and singular perturbation problems

At this point, we have discovered the importance of two characteristic length scales, the Oseen one a/Re and the Saffman one $a/\sqrt{Re_\kappa}$. If now the flow is bounded by walls, another important length scale is the distance l from the sphere centre to the nearest wall. Then comparing these various length scales allows a classification of regular and singular problems.

If both $a/\sqrt{Re_\kappa}$ and a/Re are small compared with l, this is a singular perturbation problem. Saffman considered the sub-case $a/\sqrt{Re_\kappa} \ll a/Re \ll l$ to simplify his calculation. The classification of length scales for the Saffman problem is represented schematically in Fig. 1.5.

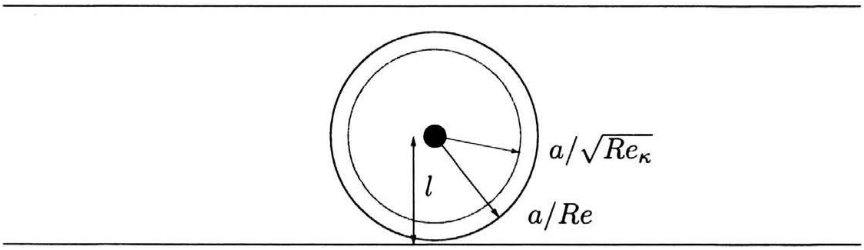

FIGURE 1.5. Singular case.

On the other hand, if $l \ll (a/\sqrt{Re_\kappa}, a/Re)$, this is a regular perturbation problem (see Fig. 1.6) since walls happen to make the second order Stokes flow regular as proven rigorously by Cox & Brenner [19] (such a case was solved in [20]).

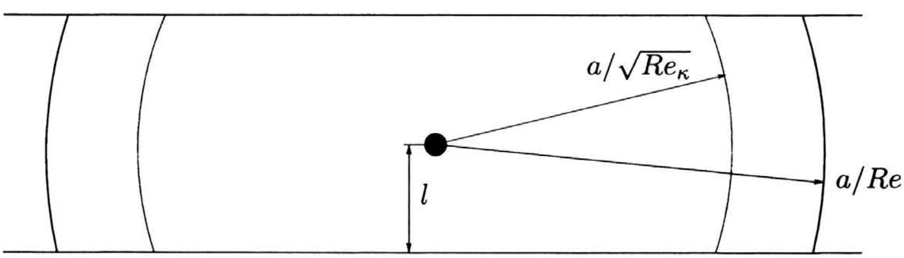

FIGURE 1.6. Regular case.

In the next Chapters, we will start by considering singular perturbation problems without walls, then regular perturbation problems with walls and finally singular perturbation problems with walls. The various theories motivated by the Segré & Silberberg experiment will be first presented shortly, classifying the problems as *regular* and *singular* ones.

1.6. Theories motivated by Segré & Silberberg experiment

Rubinow & Keller [21], following the suggestion of [9], derived a lift force similar to the Magnus force but for low Reynolds number. They showed that such a force arises from a combination of translation and rotation. Their calculation will be presented in detail in Chapter 2. This is a *singular* perturbation problem.

There is no ambient flow in [21] but Saffman [18] found that a lift force also arises from the combination of the sphere translation with an ambient shear flow. For the case that he considers, he also found that Rubinow & Keller [21] lift force is an order of magnitude smaller. This is also a *singular* perturbation problem. Saffman's work was a guide to many following papers, as we will see.

Ho & Leal [20] considered neutrally buoyant particles in a two-dimensional Poiseuille flow; they showed that a migration velocity arises from the combined effect of the local shear flow and of distant walls. They were the first ones to find limit equilibrium positions which are rather close to the experimental ones of [9]. But they considered a Poiseuille flow between parallel walls whereas the experiment [9] is concerned with a tube flow. Moreover, in their theory, the canal Reynolds number is low compared with unity whereas in experiment [9], it is of the order of 20. Their theory is based on a *regular* perturbation problem. Vasseur & Cox [22] revisited the Ho & Leal theory and, moreover, considered a more general case of a non-neutrally buoyant particle in a pure shear flow and in a Poiseuille flow between parallel walls. They found a variety of values of the lift force, depending in particular on the ratio of velocities of the particle and the ambient flow.

Segré & Silberberg experiment continued to be a motivation for many years. Indeed, Ishii & Hasimoto [23] considered the migration of a particle in Poiseuille flow in a cylindrical pipe. In their case, the pipe Reynolds number is also low. Like in [20], this perturbation problem is *regular*.

Schonberg & Hinch [24] solved again the problem for a sphere in a Poiseuille flow between parallel walls but, in their case, the canal Reynolds number may not be small (indeed, values up to around 100 are considered). They found equilibrium positions which are closer to the experimental ones [9]. The perturbation problem in this case is *singular*.

Asmolov [25] reconsidered the Poiseuille flow between parallel walls, but with an even larger canal Reynolds number (up to the order of 1000; of course with the limit that the flow should stay laminar). Then other equilibrium positions arise. The perturbation problem is again *singular*.

Various extensions of Saffman's calculation [18] were performed, in particular by Mc Laughlin [26], the perturbation problem being always *singular*.

The lift force on a particle near a wall is relevant for the departing particles in the FFF separation technique. Mc Laughlin and co-workers [27, 28] obtained various results. The perturbation problem is then *regular* because of the wall.

The most characteristic and important papers will be considered in more detail in this booklet.

Chapter 2

Lift force on a translating and rotating sphere

This Chapter is essentially a summary of the article by Rubinow & Keller [21]. The emphasis is put on matching. It is also of interest to consider a theorem giving a solution of Oseen equations which has not been much used ever since (this theorem appears in an appendix of [21]).

2.1. Problem and notation

Consider a sphere translating with velocity $\mathbf{V}$ and rotating with velocity $\mathbf{\Omega}$ in a fluid at rest. The perturbed fluid velocity and pressure satisfy the steady Navier-Stokes equations if we use a reference frame (x^*, y^*, z^*) moving with the sphere centre. The notation is depicted in Fig. 2.1. The velocity of the fluid with respect to the sphere centre, $\mathbf{V}' = -\mathbf{V}$, is pointing in the positive x^* direction. Let also $\mathbf{r}^*$ with coordinates (x^*, y^*, z^*) be the vector position of a point in the fluid and let $\mathbf{u}^*$ and p^* be the perturbed velocity and pressure. We now define dimensionless quantities, using a as a reference length and the translational velocity $\mathbf{V}' = -\mathbf{V}$ as a reference velocity. (Note that $a\mathbf{\Omega}$ would have been another possible choice. Anyway a relationship between these two scales will be imposed later). We define the dimensionless quantities:

$$x = x^*/a, \qquad y = y^*/a, \qquad z = z^*/a, \qquad \mathbf{r} = \mathbf{r}^*/a,$$

$$\mathbf{u} = \mathbf{u}^*/V, \qquad \boldsymbol{\omega} = \mathbf{\Omega} a/V, \qquad p = p^* a/(V\mu),$$

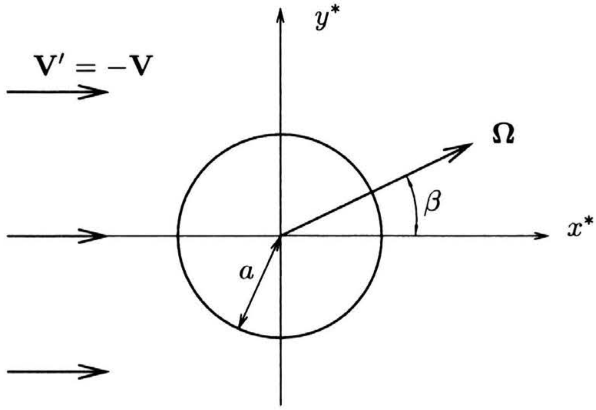

FIGURE 2.1. Notation for the flow around a translating and rotating sphere. The reference frame is attached to the sphere centre.

with $V = |\mathbf{V}|$. The Reynolds number:

$$Re = \frac{Va}{\nu}$$

is assumed to be small compared with unity. The Navier-Stokes equations and boundary conditions are then written in dimensionless form:

$$\nabla \cdot \mathbf{u} = 0, \tag{2.1a}$$

$$\nabla^2 \mathbf{u} - \nabla p = Re(\mathbf{u} \cdot \nabla)\mathbf{u}, \tag{2.1b}$$

$$r = 1 \quad : \quad \mathbf{u} = \boldsymbol{\omega} \times \mathbf{r}, \tag{2.1c}$$

$$r \to \infty \quad : \quad \mathbf{u} \to \mathbf{e}_x, \quad p \to 0, \tag{2.1d}$$

where $r = |\mathbf{r}|$ and $\mathbf{e}_x$ is the unit vector along x.

2.2. Stokes expansion

The solution is searched as an expansion in Re. First, a natural expansion is performed by keeping r of the order of unity. That is, we consider the flow field at the scale of the sphere. This is the so-called Stokes expansion:

$$\mathbf{u} = \mathbf{u}_0 + Re\, \mathbf{u}_1, \qquad p = p_0 + Re\, p_1. \tag{2.2}$$

The Navier-Stokes equations then give successively:

$$\nabla \cdot \mathbf{u}_0 = 0, \tag{2.3a}$$

$$\nabla^2 \mathbf{u}_0 - \nabla p_0 = 0, \tag{2.3b}$$

$$r = 1 \quad : \quad \mathbf{u}_0 = \boldsymbol{\omega} \times \mathbf{r}, \tag{2.3c}$$

$$\nabla \cdot \mathbf{u}_1 = 0, \tag{2.4a}$$

$$\nabla^2 \mathbf{u}_1 - \nabla p_1 = (\mathbf{u}_0 \cdot \nabla)\mathbf{u}_0, \tag{2.4b}$$

$$r = 1 \quad : \quad \mathbf{u}_1 = 0. \tag{2.4c}$$

Applying here the method of matched asymptotic expansions in a systematic way, we do not know *a priori* whether the boundary condition at infinity (2.1d) can be applied to these expansions. Indeed, this boundary condition will be replaced later by a proper matching with expansions valid in a domain far from the sphere.

2.3. Oseen expansion

The domain far from the sphere is defined by using the following stretched variables:

$$X = Re\, x, \qquad Y = Re\, y, \qquad Z = Re\, z, \qquad \mathbf{R} = Re\, \mathbf{r}.$$

The unknown velocity and pressure in terms of these variables:

$$\mathbf{U}(X, \dots) = \mathbf{u}(x, \dots), \qquad P(X, \dots) = Re^{-1} p(x, \dots),$$

then satisfy the stretched Navier-Stokes equations and boundary conditions:

$$\nabla \cdot \mathbf{U} = 0, \tag{2.5a}$$

$$\nabla^2 \mathbf{U} - \nabla P = (\mathbf{U} \cdot \nabla)\mathbf{U}, \tag{2.5b}$$

$$R \to \infty \quad : \quad \mathbf{U} \to \mathbf{e}_x, \quad P \to 0, \tag{2.5c}$$

where $R = |\mathbf{R}|$. Since $R = Ord(1)$ corresponds to a distance $r = Ord(1/Re)$ that is large compared with unity, it is appropriate to apply the boundary condition at infinity. However, it is not clear at this stage that the boundary condition on the sphere can be applied. This boundary condition will be replaced later by a proper matching with the solutions of (2.3) and (2.4) valid near the sphere.

The solution of the stretched system (2.5) is searched as an expansion for low Re with $R = Ord(1)$; this is the Oseen expansion:

$$\mathbf{U} = \mathbf{U}_0 + Re\,\mathbf{U}_1, \qquad P = P_0 + Re\,P_1.$$

The Navier-Stokes equations then give successively:

$$\nabla \cdot \mathbf{U}_0 = 0, \tag{2.6a}$$

$$\nabla^2 \mathbf{U}_0 - \nabla P_0 = \mathbf{U}_0 \cdot \nabla \mathbf{U}_0, \tag{2.6b}$$

$$R \to \infty \quad : \quad \mathbf{U}_0 \to \mathbf{e}_x; \quad P_0 \to 0, \tag{2.6c}$$

$$\nabla \cdot \mathbf{U}_1 = 0, \tag{2.7a}$$

$$\nabla^2 \mathbf{U}_1 - \nabla P_1 = \mathbf{U}_0 \cdot \nabla \mathbf{U}_1 + \mathbf{U}_1 \cdot \nabla \mathbf{U}_0, \tag{2.7b}$$

$$R \to \infty \quad : \quad \mathbf{U}_1 \to 0; \quad P_1 \to 0. \tag{2.7c}$$

The order zero equations (2.6a), (2.6b) are the full Navier-Stokes and nothing seems to be gained at this stage. Fortunately, with the boundary condition (2.6c), it has a trivial solution: $\mathbf{U}_0 = \mathbf{e}_x$, $P_0 = 0$. Then, the order 1 momentum equation (2.7b) simplifies to:

$$\nabla^2 \mathbf{U}_1 - \nabla P_1 = \frac{\partial U_1}{\partial X}. \tag{2.8}$$

This is the classical Oseen equation. Since it is linear, it can be solved reasonably easily.

2.4. Matching and Stokes solution at order 0

Stokes approximation is valid for $r = Ord(1)$ and Oseen approximation valid for $R = Ord(1)$ that is $r = Ord(1/Re)$. In general, one expects (see Sec. A.2.2) both solutions to be valid in some intermediate region where $Ord(1) < Ord(r) < Ord(1/Re)$. But here, it happens that Stokes solution is uniformly valid. Thus, we simply use van Dyke matching principle:

$$\lim_{r\to\infty} \mathbf{u}_0 = \lim_{R\to 0} \mathbf{U}_0.$$

The result for the order 0 Stokes term simply amounts to the classical boundary condition at infinity:

$$r \to \infty : \mathbf{u}_0 \to \mathbf{e}_x. \tag{2.9}$$

That is, the problem is regular at this order.

The solution of (2.3a) (2.3b) with boundary conditions (2.3c) (2.9) is found from linearity of the Stokes equations (2.3a) (2.3b) by simply superimposing classical solutions for the translation and rotation of a sphere:

$$\begin{aligned} \mathbf{u}_0 &= \mathbf{e}_x - \frac{3}{4}\mathbf{e}_x \cdot \left(\frac{\mathbf{I}}{r} + \frac{\mathbf{rr}}{r^3}\right) - \frac{1}{4}\mathbf{e}_x \cdot \left(\frac{\mathbf{I}}{r^3} - 3\frac{\mathbf{rr}}{r^5}\right) \\ &\quad + \frac{\boldsymbol{\omega} \times \mathbf{r}}{r^3}, \qquad (2.10a) \\ p_0 &= -\frac{3}{2}\mathbf{e}_x \cdot \frac{\mathbf{r}}{r^3}. \qquad (2.10b) \end{aligned}$$

2.5. Solution of Oseen (order 1) equation

We have seen that the order 1 Oseen system consists of (2.7) in which the momentum equation (2.7b) simplifies to the classical Oseen equation (2.8):

$$\begin{aligned} \boldsymbol{\nabla} \cdot \mathbf{U}_1 &= 0, \\ \nabla^2 \mathbf{U}_1 - \boldsymbol{\nabla} P_1 &= \frac{\partial U_1}{\partial X}, \\ R \to \infty &: \quad \mathbf{U}_1 \to 0; \quad P_1 \to 0. \end{aligned}$$

The solution is found as:

$$\begin{aligned} P_1 &= \frac{\partial \phi}{\partial X}, \\ \mathbf{U}_1 &= -\boldsymbol{\nabla}\phi + \mathbf{W}, \end{aligned}$$

where

$$\begin{aligned} \boldsymbol{\nabla} \cdot \mathbf{W} &= 0, \\ \frac{\partial \mathbf{W}}{\partial X} &= \nabla^2 \mathbf{W}. \end{aligned}$$

W is found due to the following theorem by Rubinow & Keller ([21], Appendix).

Theorem 2.1: *There are two scalar functions* ψ *and* χ *such that:*

$$\mathbf{W} = \mathbf{e}_x \times \boldsymbol{\nabla}\psi + \boldsymbol{\nabla} \times (\mathbf{e}_x \times \boldsymbol{\nabla}\chi),$$

and

$$\nabla^2\psi = \frac{\partial\psi}{\partial X}, \qquad \nabla^2\chi = \frac{\partial\chi}{\partial X}.$$

Another way of writing it, with $\chi' = \frac{\partial\chi}{\partial X}$ *such that* $\nabla^2\chi' = \frac{\partial\chi'}{\partial X}$, *is:*

$$\mathbf{W} = \boldsymbol{\nabla}\chi' + \left(-\chi', -\frac{\partial\psi}{\partial Z}, \frac{\partial\psi}{\partial Y}\right).$$

The solution in the present case is obtained by using a particular case of the theorem (a case already mentioned by Lamb [29]) where $\psi = 0$. Then:

$$\phi = \frac{A}{R}, \qquad \chi' = \frac{B}{R}\exp\left[\frac{1}{2}(X - R)\right],$$

and the solution for the pressure and velocity terms is:

$$\begin{aligned} P_1 &= \frac{\partial\phi}{\partial X}, \\ \mathbf{U}_1 &= -\boldsymbol{\nabla}\phi + \mathbf{W} = \boldsymbol{\nabla}(-\phi + \chi') \\ &= A\frac{\mathbf{R}}{R^3} - B\frac{\mathbf{R}}{R^3}e^{\frac{1}{2}(X-R)} + \cdots \end{aligned}$$

where the constants A and B have to be found by matching.

2.6. Matching Oseen order 1 expansion with Stokes order 0 expansion

Applying van Dyke's matching principle (see Sec. A.2.1), change variable $\mathbf{R} = Re\,\mathbf{r}$ in the Oseen expansion and then expand it up to $Ord(Re)$ for small Re at $r = Ord(1)$ (Stokes expansion):

$$\mathbf{U}_0 + Re\mathbf{U}_1 = \mathbf{e}_x + \frac{A - B}{Re}\frac{\mathbf{r}}{r^3} + \mathbf{Ord(1)\ terms} + O(Re).$$

Next, match with Stokes solution at order 0, Eq. (2.10a):

- The matching of $\mathbf{e}_x$ was already done at order 0.
- The **term in** $1/Re$ is blowing up when $Re \to 0$; it should disappear, thus $A = B$.

- The other **Ord(1) terms**, not detailed here, match with Stokes solution provided $B = 3/2$.

Thus matching with Stokes solution at order 0 gives $A = B = 3/2$, so that:

$$\mathbf{U}_1 = \frac{3}{2}\frac{\mathbf{R}}{R^3} - \frac{3}{4}\frac{\mathbf{e}_x}{R}\exp\left[\frac{1}{2}(X-R)\right] - \frac{3}{4}\mathbf{R}\left(\frac{1}{R^2} - \frac{2}{R^3}\right)\exp\left[\frac{1}{2}(X-R)\right],$$

$$P_1 = -\frac{3}{2}\frac{X}{R^3}.$$

2.7. Stokes approximation at order 1

Next, we solve the system (2.4), which is recalled here:

$$\nabla \cdot \mathbf{u}_1 = 0, \tag{2.11a}$$

$$\nabla^2 \mathbf{u}_1 - \nabla p_1 = (\mathbf{u}_0 \cdot \nabla)\mathbf{u}_0, \tag{2.11b}$$

$$r = 1 \quad : \quad \mathbf{u}_1 = 0. \tag{2.11c}$$

in which $\mathbf{u}_0$ was calculated in (2.10a). Taking the divergence of the momentum equation (2.11b) and using the continuity equation (2.11a), we obtain a Poisson equation for p_1:

$$\begin{aligned} \nabla^2 p_1 &= -\nabla \cdot (\mathbf{u}_0 \cdot \nabla)\mathbf{u}_0 \\ &= \frac{9}{8}\left[-\frac{1}{r^4} + \frac{1}{r^8} + x^2\left(\frac{4}{r^2} - \frac{6}{r^8} + \frac{2}{r^{10}}\right)\right] \\ &\quad -\frac{3}{2}\omega\, z \sin\beta\left(\frac{1}{r^6} - \frac{1}{r^8}\right) + 4\frac{\omega^2}{r^6} - \frac{(\boldsymbol{\omega}\cdot\mathbf{r})^2}{r^8}. \end{aligned}$$

Let a particular solution of this equation be p_{10}. Then, there is an associated velocity field $\mathbf{u}_{10}$ such that:

$$\begin{aligned} \nabla \cdot \mathbf{u}_{10} &= 0, \\ \nabla^2 \mathbf{u}_{10} &= \nabla p_{10} + (\mathbf{u}_0 \cdot \nabla)\mathbf{u}_0. \end{aligned}$$

The unknown solution $\mathbf{u}_1$ is found as:

$$\mathbf{u}_1 = \mathbf{u}_{10} + \mathbf{u}_{11}, \qquad p_1 = p_{10} + p_{11},$$

in which the velocity $\mathbf{u}_{11}$ and associated pressure p_{11} should satisfy:

$$\begin{aligned} \nabla \cdot \mathbf{u}_{11} &= 0, \\ \nabla^2 \mathbf{u}_{11} &= \nabla p_{11}, \\ r = 1 \quad &: \quad \mathbf{u}_{11} = -\mathbf{u}_{10}. \end{aligned}$$

This last problem is simply a Stokes flow problem with specified conditions on a boundary. Lamb's [29] general expression of the solution of Stokes equations can then be used to find $\mathbf{u}_{11}$, p_{11}. Then the formal solution for $\mathbf{u}_1$, p_1 is obtained. Details may be found in [21].

2.8. Matching Oseen order 1 expansion with Stokes order 1 expansion

Using again van Dyke matching principle, we:

- rewrite Oseen expansion $\mathbf{U}_0 + Re\,\mathbf{U}_1$ in Stokes variable and expand;
- compare with Stokes expansion $\mathbf{u}_0 + Re\,\mathbf{u}_1$.
  That is, not only the order 1 terms have to be matched, but the whole expansions.

2.9. Drag, lift and torque

After having calculated the fluid velocity and pressure, the dimensional stress on the sphere can be calculated with the following expression [29]:

$$\mathbf{f}^* = \boldsymbol{\sigma}^* \cdot \mathbf{n} = \frac{V\mu}{a}\left[-\frac{\mathbf{r}^*}{r^*}p^* + \left(\frac{\partial}{\partial r^*} - \frac{1}{r^*}\right)\mathbf{u}^* + \frac{1}{r^*}\nabla(\mathbf{r}^* \cdot \mathbf{u}^*)\right]$$

where $\boldsymbol{\sigma}^*$ is the stress tensor and $\mathbf{n}$ is the normal unit vector pointing into the fluid. Then integrating the stress on the sphere surface gives the force on the sphere:

$$\begin{aligned} \mathbf{F}^* &= \int_S \mathbf{f}^*\, dS \\ &= -\,6\pi a\mu\mathbf{V}\left(1+\frac{3}{8}Re\right) \quad \textbf{(Stokes drag force plus Oseen correction)} \\ &\quad + \pi a\mu\, Re\, \boldsymbol{\omega} \times \mathbf{V} \quad \textbf{(Rubinow \& Keller lift force)} \\ &\quad + o(a\mu V\, Re). \end{aligned}$$

The correction to the drag is the same as the one obtained for a non-rotating sphere by Oseen [16] [1]. The essential result of Rubinow & Keller is a lift force, that is a force perpendicular to the sphere translational velocity. From the expression of the Reynolds number, the lift force may also be rewritten as

$$\pi a^3 \rho \boldsymbol{\Omega} \times \mathbf{V}.$$

Surprisingly, it does not contain the viscosity. One may think that it is a purely inertial term but it is different from the Magnus force which is for dominant inertial effects. The present force can rather be understood as a second term $O(\mu^0)$ of an expansion for large viscosity μ.

Rubinow & Keller also derived the torque on the sphere:

$$\begin{aligned} \mathbf{C}^* &= \int_S \mathbf{r}^* \times \mathbf{f}^* \, dS \\ &= -8\pi a^3 \mu \boldsymbol{\Omega}(1 + o(Re)), \end{aligned}$$

viz. this is the classical result for Stokes flow (due to Kirchoff, cf. [29] § 334) and there is no inertial correction at this order.

The rest of the article [21] is discussing Segré-Silberberg experiment, but following papers are more relevant to this problem.

[1] Note that further terms have been calculated for the purely translational problem [30].

Chapter 3

Lift force on a sphere translating and freely rotating in a shear flow

This Chapter is based on Saffman's article [18]. This article is important for two reasons. First, its new exact result for the lift force has been exploited in many applications. Secondly, the main ideas of its calculation technique have been used for various singular perturbation problems until today.

3.1. Problem and notation

Consider a sphere translating with velocity $\mathbf{V}$ relative to an ambient (unperturbed) shear flow with shear rate κ. The shear flow and sphere velocities

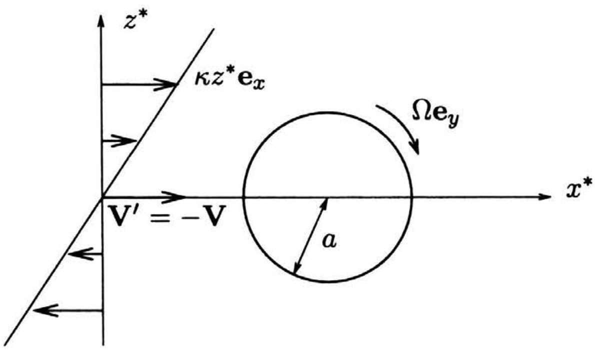

FIGURE 3.1. Translating sphere.

are in the same direction, say x^*. Like in Chapter 2, using a reference frame moving with the sphere centre allows to use the steady Navier-Stokes equations. The system of coordinates and notation is shown in Fig. 3.1.

The sphere is also rotating with velocity $\Omega \mathbf{e}_y$ (where the unit vector $\mathbf{e}_y$ is pointing into the figure). Let $\mathbf{V}' = V'\mathbf{e}_x = -\mathbf{V}$. In the chosen frame, the unperturbed flow velocity or velocity at infinity is $\mathbf{u}^* \to (V' + \kappa z^*)\mathbf{e}_x$ and the fluid velocity on the sphere is $\mathbf{u}^* = \Omega \mathbf{e}_y \times \mathbf{r}^*$.

Here, two Reynolds numbers appear:

$$Re = \frac{V'a}{\nu}, \qquad Re_\kappa = \frac{\kappa a^2}{\nu}.$$

Note that Re may here be positive or negative. Both Re and Re_κ are assumed to be small compared with unity. Choosing V' as a reference velocity (we will see later that κa will appear anyway through Re_κ); let $\mathbf{u} = \mathbf{u}^*/V'$ and $\omega = \Omega a/V'$. Choosing a as a reference length; let $\mathbf{r} = \mathbf{r}^*/a$. Let the dimensionless force $\mathbf{F}$ and torque $\mathbf{C}$ be defined in terms of the dimensional ones $\mathbf{F}^*$ and $\mathbf{C}^*$ by: $\mathbf{F}^* = a\mu V'\mathbf{F}$ and $\mathbf{C}^* = a^3\mu\Omega\mathbf{C}$, respectively. Expanding for small Re, we expect to find the force on the sphere:

$$\mathbf{F} = \mathbf{F}_0 + Re\,\mathbf{F}_1.$$

3.2. Stokes expansion and order 0 Stokes solution

We expand the fluid velocity and pressure for $Re \ll 1$ keeping $r = Ord(1)$, that is the Stokes expansion:

$$\mathbf{u} = \mathbf{u}_0 + Re\,\mathbf{u}_1, \qquad p = p_0 + Re\,p_1.$$

Like in the Rubinow & Keller case, the order 0 Oseen expansion is trivial and matching with it only gives the expected boundary condition at infinity for the order 0 Stokes solution. Using classical solutions of the Stokes equations, we then obtain:

$$\begin{aligned}\mathbf{u}_0 \;=\;& \mathbf{e}_x - \frac{3}{4}\mathbf{e}_x \cdot \left(\frac{\mathbf{I}}{r} + \frac{\mathbf{rr}}{r^3}\right) - \frac{1}{4}\mathbf{e}_x \cdot \left(\frac{\mathbf{I}}{r^3} - 3\frac{\mathbf{rr}}{r^5}\right) + \frac{Re_\kappa}{Re} z\mathbf{e}_x \\ & + \frac{1}{2}\frac{Re_\kappa}{Re}\left\{-5\frac{xz\mathbf{r}}{r^5}\left(1 - \frac{1}{r^2}\right) - \frac{1}{r^3}(\mathbf{e}_x z - \mathbf{e}_z x) - \frac{1}{r^5}(\mathbf{e}_x z + \mathbf{e}_z x)\right\} \\ & + \Omega\left\{\frac{1}{r^3}(\mathbf{e}_x z - \mathbf{e}_z x)\right\} \end{aligned} \tag{3.1}$$

and the classical Faxen results, here written in dimensional form, for the drag force on the sphere:

$$\mathbf{F}^* = 6\pi a\mu V'\mathbf{e}_x,$$

and for the torque:

$$\mathbf{C}^* = 8\pi a^3\mu\left(\frac{1}{2}\kappa - \Omega\right)\mathbf{e}_y.$$

3.3. Order 1 Stokes expansion

3.3.1. Expression for the force in terms of some integrals

The order 1 Stokes momentum equation is:

$$\nabla^2\mathbf{u}_1 - \boldsymbol{\nabla}p_1 = (\mathbf{u}_0\cdot\boldsymbol{\nabla})\mathbf{u}_0$$

or in terms of the stress tensor $\boldsymbol{\sigma}_1$ at order 1 and using the continuity equation at order 0, $\boldsymbol{\nabla}\cdot\mathbf{u}_0 = 0$:

$$\boldsymbol{\nabla}\cdot\boldsymbol{\sigma}_1 = \boldsymbol{\nabla}\cdot(\mathbf{u}_0\mathbf{u}_0).$$

The order 1 term of the expansion of the dimensionless force on the sphere is:

$$\mathbf{F}_1 = \int\limits_{r=1}\boldsymbol{\sigma}_1\cdot\mathbf{n}\,dS.$$

Thus, using the divergence theorem on a domain between the sphere of radius 1 and a large sphere of radius $\mathcal{R}$ we get:

$$\mathbf{F}_1 = \int\limits_{r=\mathcal{R}}\boldsymbol{\sigma}_1\cdot\mathbf{n}\,dS - \int\limits_{r=\mathcal{R}}(\mathbf{u}_0\mathbf{u}_0)\cdot\mathbf{n}\,dS + \int\limits_{r=1}(\mathbf{u}_0\mathbf{u}_0)\cdot\mathbf{n}\,dS. \tag{3.2}$$

Since $\mathbf{u}_0 = \omega\mathbf{e}_y\times\mathbf{r}$ on the sphere $r = 1$, then $\mathbf{u}_0\cdot\mathbf{n} = 0$ and the last integral vanishes.

Instead of calculating the full solution $(\mathbf{u}_1, p_1)$ of the order 1 Stokes equation, the main idea of [18] is to express the unknown $\mathbf{F}_1$ in terms of some integrals and then perform the calculations on these integrals.

For that purpose, using the identity:

$$\int\limits_{r=\mathcal{R}}\boldsymbol{\nabla}\cdot\boldsymbol{\phi}\,dS = \frac{d}{d\mathcal{R}}\int\limits_{r\le\mathcal{R}}\boldsymbol{\nabla}\cdot\boldsymbol{\phi}\,dV = \frac{d}{d\mathcal{R}}\int\limits_{r=\mathcal{R}}\boldsymbol{\phi}\mathbf{n}\,dS,$$

the deviatoric (viscous) part of the contribution $\int_{r=\mathcal{R}} \boldsymbol{\sigma}_1 \cdot \mathbf{n}\, dS$ to $\mathbf{F}_1$ in equation (3.2) is expressed as:

$$\int_{r=\mathcal{R}} (\boldsymbol{\nabla}\mathbf{u}_1 +^t \boldsymbol{\nabla}\mathbf{u}_1) \cdot \mathbf{n}\, dS = \mathcal{R}\frac{d}{d\mathcal{R}} \int_{r=\mathcal{R}} \frac{\mathbf{u}_1}{\mathcal{R}}\, dS - \int_{r=\mathcal{R}} \frac{\mathbf{u}_1}{\mathcal{R}}\, dS.$$

Thus the expression (3.2) for the unknown $\mathbf{F}_1$ becomes:

$$\mathbf{F}_1 = -\int_{r=\mathcal{R}} \frac{p_1\mathbf{r}}{\mathcal{R}}\, dS + \mathcal{R}\frac{d}{d\mathcal{R}} \int_{r=\mathcal{R}} \frac{\mathbf{u}_1}{\mathcal{R}}\, dS - \int_{r=\mathcal{R}} \frac{\mathbf{u}_1}{\mathcal{R}}\, dS - \int_{r=\mathcal{R}} \frac{(\mathbf{u}_0\mathbf{u}_0)\cdot\mathbf{r}}{\mathcal{R}}\, dS, \quad (3.3)$$

so that $\mathbf{F}_1$ is expressed in terms of only two unknown integrals on a large sphere.

3.3.2. Solutions for the two unknown integrals

Two coupled differential equations may be derived for the two unknown integrals [18]:

$$\begin{aligned}
\mathcal{R}\frac{d^2}{d\mathcal{R}^2} \int_{r=\mathcal{R}} \frac{\mathbf{u}_1}{\mathcal{R}}\, dS - \frac{d}{d\mathcal{R}} \int_{r=\mathcal{R}} \frac{p_1\mathbf{r}}{\mathcal{R}}\, dS &= \int_{r=\mathcal{R}} (\mathbf{u}_0 \cdot \boldsymbol{\nabla})\mathbf{u}_0\, dS \\
&= \sum_n \mathbf{a}_n \mathcal{R}^n, \\
-\mathcal{R}\frac{d^2}{d\mathcal{R}^2} \int_{r=\mathcal{R}} \frac{p_1\mathbf{r}}{\mathcal{R}}\, dS + 2\frac{d}{d\mathcal{R}} \int_{r=\mathcal{R}} \frac{p_1\mathbf{r}}{\mathcal{R}}\, dS &= \int_{r=\mathcal{R}} \mathbf{r}\boldsymbol{\nabla} \cdot (\mathbf{u}_0 \cdot \boldsymbol{\nabla})\mathbf{u}_0\, dS \\
&= \sum_n \mathbf{b}_n \mathcal{R}^n.
\end{aligned}$$

The last sums are obtained from the expression (3.1) of $\mathbf{u}_0$ which is of the form $\mathbf{u}_0 = (Re_\kappa/Re)z\mathbf{e}_x + \mathbf{e}_x + O(1/r) + \cdots$ and it may be shown that the only non zero $\mathbf{a}_n$ coefficients are for $n \leq 2$ and the only non zero $\mathbf{b}_n$ are for $n \leq 1$.

Solving the system of two equations for the two unknown integrals, we obtain:

$$\int\limits_{r=\mathcal{R}} \frac{p_1 \mathbf{r}}{\mathcal{R}}\, dS = \sum_{n\neq -2,-1} \mathbf{b}_n \frac{\mathcal{R}^{n+1}}{(n+1)(n+2)} + \mathbf{A} + \mathbf{B}\mathcal{R}^3, \tag{3.4}$$

$$\int\limits_{r=\mathcal{R}} \frac{\mathbf{u}_1}{\mathcal{R}}\, dS = \sum_{n\neq -1,0} \mathbf{a}_n \frac{\mathcal{R}^{n+1}}{n(n+1)} + \sum_{n\neq -2,-1,0} \mathbf{b}_n \frac{\mathcal{R}^{n+1}}{n(n+1)(n+2)} + \mathbf{C}\mathcal{R} + \mathbf{D}, \tag{3.5}$$

where $\mathbf{A}, \mathbf{B}, \mathbf{C}, \mathbf{D}$ denote here constant vectors to be determined.

Since $\mathbf{a}_2 \neq \mathbf{0}$, then $\mathbf{u}_1 = O(\mathcal{R}^2)$ does not vanish at infinity. Thus the perturbation problem is singular and the condition at infinity should be replaced by matching with a solution valid in a region far from the sphere.

3.3.3. Expression for the force at order 1

The coefficients $\mathbf{A}, \mathbf{D}$ are obtained in terms of the other coefficients from:

- the order 1 Stokes equation,
- the boundary condition $\mathbf{u}_1 = 0$ on the sphere $r = 1$.

The coefficients $\mathbf{B}, \mathbf{C}$ should be obtained by matching.

The result for the order 1 contribution to the force is from the expression (3.3) and the values (3.4) and (3.5) of the integrals:

$$\mathbf{F}_1 = \sum_n \left\{ \mathbf{a}_n \frac{3}{2n} + \mathbf{b}_n \frac{3-n}{2n(n-2)} \right\} + \frac{3}{4}\mathbf{B} + \frac{3}{2}\mathbf{C}. \tag{3.6}$$

The $\mathbf{a}_n$ and $\mathbf{b}_n$ are calculated from Stokes flow. The $\sum$ term gives the following contribution to the component of $\mathbf{F}_1$ along z, in dimensional form, that is to F^*_{1z}:

$$-\pi\rho a^3 \Omega V' - \frac{11}{8}\pi\rho a^3 \kappa V'.$$

The first term is the Rubinow & Keller's lift force $\pi\rho a^3 \mathbf{\Omega} \times \mathbf{V}$ for a sphere translating with velocity $\mathbf{V} = -\mathbf{V}'$. Another contribution, indeed the most interesting one, comes from the terms in $\mathbf{B}, \mathbf{C}$ and will be found by matching.

3.4. Order 1 (Oseen like) Saffman expansion

3.4.1. Scaling

We have seen earlier that the non-linear term $\rho(\mathbf{u}^* \cdot \boldsymbol{\nabla})\mathbf{u}^*$ is of the order of the viscous terms $\mu\nabla^2\mathbf{u}^*$ in shear flow for $r^* \sim a/\sqrt{Re_\kappa}$, the "Saffman distance".

In more detail: introduce the expansions $\mathbf{u} = \mathbf{e}_x + (Re_\kappa/Re)z\mathbf{e}_x + Re\mathbf{U}_1$ and $p = ReP_1$ into the Navier-Stokes equation

$$Re(\mathbf{u} \cdot \boldsymbol{\nabla})\mathbf{u} = -\boldsymbol{\nabla}p + \nabla^2\mathbf{u}.$$

At large distances, the z term is preponderant in the inertia term:

$$Re\left(\frac{Re_\kappa}{Re}z\right)\mathbf{e}_x \cdot \boldsymbol{\nabla}\mathbf{u} = Re_\kappa z\frac{\partial}{\partial x}\mathbf{u} = Re_\kappa z\frac{\partial}{\partial x}(Re\mathbf{U}_1).$$

The inertia term is of the order of the viscous term $\nabla^2\mathbf{u} = \nabla^2(Re\mathbf{U}_1)$ at distances $Ord(1/\sqrt{Re_\kappa})$.

Thus we use the following stretched variable:

$$\tilde{X} = \sqrt{Re_\kappa}\,x\,, \quad \tilde{Y} = \sqrt{Re_\kappa}\,y\,, \quad \tilde{Z} = \sqrt{Re_\kappa}\,z\,, \quad \tilde{\mathbf{R}} = \sqrt{Re_\kappa}\,\mathbf{r}\,, \quad \tilde{R} = |\tilde{\mathbf{R}}|\,.$$

The "Saffman limit" is now the limit $Re \to 0$ while keeping $\tilde{R} = Ord(1)$. We also rescale the velocity $\mathbf{U}_1$ and pressure P_1 so as to keep as many terms as possible in this limit:

$$\tilde{\mathbf{U}}_1 = \frac{Re}{\sqrt{Re_\kappa}}\mathbf{U}_1, \qquad \tilde{P}_1 = \frac{Re}{Re_\kappa}P_1.$$

3.4.2. Saffman (Oseen like) equation

In the Saffman limit, the Navier-Stokes equations become:

$$\left(\frac{Re}{\sqrt{Re_\kappa}} + \tilde{Z}\right)\frac{\partial\tilde{\mathbf{U}}_1}{\partial\tilde{X}} + \tilde{W}_1\mathbf{e}_x = -\tilde{\boldsymbol{\nabla}}\tilde{P}_1 + \tilde{\nabla}^2\tilde{\mathbf{U}}_1, \tag{3.7a}$$

$$\tilde{\boldsymbol{\nabla}} \cdot \tilde{\mathbf{U}}_1 = 0, \tag{3.7b}$$

where $\tilde{W}_1$ denotes the $\tilde{Z}$ component of $\tilde{\mathbf{U}}_1$. Since these equations are valid far from the sphere, we may apply the boundary condition: for $\tilde{R} \to \infty$, $\tilde{\mathbf{U}}_1 \to 0$. On the other hand for $\tilde{R} \to 0$, the solution should match the result of the Stokes expansion. In particular, it should match the $Ord(1/r)$ terms, viz. the Stokeslet. Saffman's original approach introduces this condition into the order 1 equation (3.7a) as the Dirac delta function:

$$\left(\frac{Re}{\sqrt{Re_\kappa}} + \tilde{Z}\right)\frac{\partial \tilde{\mathbf{U}}_1}{\partial \tilde{X}} + \tilde{V}_z \mathbf{e}_x = -\tilde{\boldsymbol{\nabla}}\tilde{P}_1 + \tilde{\nabla}^2\tilde{\mathbf{U}}_1 - 6\pi\mathbf{e}_x\delta(\tilde{\mathbf{R}}), \qquad (3.8)$$

viz. the term with δ is the Stokeslet.

3.4.3. Expression for the velocity in Saffman region

From the solution of this equation, the expression for the velocity may be written as:

$$\tilde{\mathbf{U}}_1 = \tilde{\mathbf{U}}_S + \tilde{\mathbf{U}}_H$$

where $\tilde{\mathbf{U}}_S$ is the Stokeslet velocity and $\tilde{\mathbf{U}}_H$ is regular, viz.:

$$\tilde{\mathbf{U}}_H = H_1(\tilde{\mathbf{R}}) + \tilde{R}H_2(\tilde{\mathbf{R}}) + \cdots,$$

and the H_i's are homogeneous of degree 0. For $\tilde{R} \to 0$, the leftover term in $\tilde{\mathbf{U}}_H$ is a constant: $\tilde{\mathbf{U}}_H(0) = H_1(0)$.

3.5. Order 1 matching

For the order 1 Stokes flow, the constant $H_1(0)$ corresponds to a uniform flow at infinity, which will give the unknown force on the sphere. We apply van Dyke's matching principle:

- Saffman's expansion:

$$\mathbf{u} = \mathbf{e}_x + \frac{\sqrt{Re_\kappa}}{Re}\tilde{Z}\mathbf{e}_x + \sqrt{Re_\kappa}(\tilde{\mathbf{U}}_S + \tilde{\mathbf{U}}_H),$$

- rewritten in the Stokes variable:

$$\mathbf{u} = \mathbf{e}_x + \frac{Re_\kappa}{Re}Z\mathbf{e}_x + Re\left(\mathbf{U}_S + \underline{\mathbf{U}_H(\sqrt{Re_\kappa}\,\mathbf{R})}\right) + \underbrace{O(\sqrt{Re_\kappa})}.$$

- The order 1 Stokes expansion (in what follows, $\mathbf{u}_{PD} + \mathbf{u}_{SS} + \mathbf{u}_{PQ}$ represent the terms in $1/r^2, 1/r^4$):

$$\mathbf{u} = \mathbf{e}_x + \frac{Re_\kappa}{Re}Z\mathbf{e}_x + \mathbf{u}_S + \underbrace{\mathbf{u}_{PD} + \mathbf{u}_{SS} + \mathbf{u}_{PQ}} + Re\,\underline{\mathbf{u}_1}.$$

The Stokeslet term $Re\mathbf{U}_S$ matches $\mathbf{u}_S$. Since the under-braced terms $\underbrace{\mathbf{u}_{PD} + \mathbf{u}_{SS} + \mathbf{u}_{PQ}}$ vanish at infinity, the only term that can match to the underlined constant term $\underline{\mathbf{U}_H(0)}$ when $R \to 0$ is $\underline{\mathbf{u}_1}$. As a consequence:

$$\int\limits_{r=\mathcal{R}} \frac{\mathbf{u}_1}{\mathcal{R}}\, dS = \int\limits_{r=\mathcal{R}} \frac{\mathbf{u}_H(0)}{\mathcal{R}}\, dS.$$

Results follow for the constants: $\mathbf{B} = 0$ and $\mathbf{C}$ is found.

3.6. Solution of order 1 Saffman equation

The solution of (3.8) with (3.7b) is found with a three-dimensional Fourier transform. To determine $\mathbf{C}$, the needed regular part in $\tilde{R} = 0$ is calculated as:

$$\tilde{\mathbf{U}}_H(0) = \lim_{\tilde{R}\to 0} (\tilde{\mathbf{U}}_1 - \tilde{\mathbf{U}}_S) = \lim_{\tilde{R}\to 0} \int (\hat{\tilde{\mathbf{U}}}_1 - \hat{\tilde{\mathbf{U}}}_S) e^{i\mathbf{k}\cdot\tilde{\mathbf{R}}}\, d\mathbf{k} = \int (\hat{\tilde{\mathbf{U}}}_1 - \hat{\tilde{\mathbf{U}}}_S)\, d\mathbf{k} \tag{3.9}$$

that is, there is no need to calculate the full solution in real space.

3.7. Saffman lift force

Saffman studied the case $Re \ll \sqrt{Re_\kappa} \ll 1$. Then the Oseen like term, viz. the term in $(Re/\sqrt{Re_\kappa})$ in the left-hand-side of (3.8), drops out in the equation for the Saffman region. The lift force (z component of the second order term in the force on the sphere) is due to shear flow:

$$F_z^* = 6.46\, a\mu V' \sqrt{Re_\kappa} = 6\pi a\mu V'(0.343\sqrt{Re_\kappa}).$$

Note that there is an error in Saffman's (1965) original paper: see the corrigendum (1968) [18]. Recall that V' is the undisturbed fluid velocity with respect to the sphere centre. Cases in which this velocity does not vanish may be e.g.:

- a non-neutrally buoyant particle in a vertical undisturbed fluid velocity;
- a solid particle in a gas, with a high enough Stokes number (ratio of the characteristic time for accelerating the particle to a characteristic time of the carrier flow), so that the particle may have a different velocity from that of the carrier gas.

If the sphere is lagging the flow, that is if $V' > 0$, the Saffman lift force is pushing the sphere towards the positive z direction, that is towards the streamlines with a higher velocity. On the other hand, if the sphere is faster than the local flow, that is if $V' < 0$, the force is towards the streamlines with a lower velocity.

The Saffman force is much larger than the Rubinow & Keller force. Note that the sphere is yet rotating.

3.8. Various extensions of Saffman's result

3.8.1. Sphere moving in any direction

Harper & Chang [31] considered also the case $Re \ll \sqrt{Re_\kappa} \ll 1$ like Saffman, but for the more general case of a spherical particle moving with a velocity in any direction $\mathbf{V} = (V_x, V_y, V_z)$ in a shear flow with rate of shear κ, plane of shear (x^*, z^*) and direction x^*. In the Saffman case, the lift force is due to a velocity in the x direction and eventually gives a velocity in the z direction which is of an order $\sqrt{Re_\kappa}$ smaller. But here, all velocity components V_x, V_y, V_z are of the same order. Miyazaki, Bedeaux & Bonet Avalos [32] found the same analytical results as in [31] but their numerical results differ considerably from [31]. The force on the particle is then from [32]:

$$\begin{aligned}
F_x^* &= 6\pi a\mu \left[\left(1 + 0.0735\sqrt{Re_\kappa}\right)([V_\infty]_0 - V_x) - 0.944\sqrt{Re_\kappa})V_z\right], \\
F_y^* &= -6\pi a\mu \left(1 + 0.577\sqrt{Re_\kappa}\right) V_y, \\
F_z^* &= 6\pi a\mu \left[0.343\sqrt{Re_\kappa}([V_\infty]_0 - V_x) - \left(1 + 0.327\sqrt{Re_\kappa}\right) V_z\right],
\end{aligned}$$

where $[V_\infty]_0$ is the value of the undisturbed flow V_∞ taken at the sphere centre. Harper & Chang and Miyazaki *et al* recover Saffman's lift force and find other coefficients for the lift force when the sphere is moving perpendicular to the shear flow. They also find Oseen like corrections to the drag, but involving $\sqrt{Re_\kappa}$.

3.8.2. Fluid inertia contribution to the stress tensor of a suspension

Lin, Peery & Schowalter [33] considered a neutrally buoyant freely rotating sphere embedded in a pure shear flow. They derived the sphere rotational velocity:

$$\Omega = \frac{\kappa}{2}\left(1 - 0.3076\,(Re_\kappa)^{3/2}\right).$$

Moreover, they showed that for a dilute suspension the fluid inertia gives a correction to Einstein's expression for the fluid viscosity, as well as normal stresses.

3.8.3. Lift force in other flow fields

Herron, Davis & Bretherton [34], following the original work of Childress [35] found components of force like in [31], but for a sphere in a centrifuge.

Drew [36] also found similar relationships for a sphere in a 2D pure straining motion and a 2D rotational motion.

More details about the preceding extensions of Saffman's results may be found in [37].

3.8.4. Lift for concurrent translational and shear flow effects

More recently, Mc Laughlin [26] considered the *Oseen like term* neglected by Saffman. That is, he considered the general case in which translational and shear flow inertial effects may be of the same order of magnitude, viz. $Re \sim \sqrt{Re_\kappa} \ll 1$, so that all inertial terms are kept on the left-hand-side of (3.8). He calculated the inertial migration velocity directly from Saffman's expression (3.9) which appears like an entrainment velocity for the sphere (Note that the lift force is $6\pi a\mu$ times this velocity, at this order in Reynolds number). His results for the dimensional migration velocity in terms of $\epsilon = \sqrt{Re_\kappa}/Re$ are:

$$V_m = \frac{3}{2\pi^2} V' \sqrt{Re_\kappa}\, J = \begin{cases} \text{if } \epsilon \gg 1 & : \ J = 2.255 - 0.6463/\epsilon^2, \\ \text{if } \epsilon \sim 1 & : \ \text{cf. Table in [26]}, \\ \text{if } \epsilon \ll 1 & : \ J = -32\,\pi^2\epsilon^5 \ln(1/\epsilon^2) \\ & \quad \text{quite small for } \epsilon < 0.2 \text{ (Oseen case).} \end{cases} \tag{3.10}$$

If the velocity V' of the fluid relative to the sphere is positive, then the migration velocity V_m is moving the sphere toward increasing unperturbed velocities. Saffman's result is recovered from the formula for large ϵ when $\epsilon \to \infty$. A plot of the normalized migration velocity J versus ϵ is shown

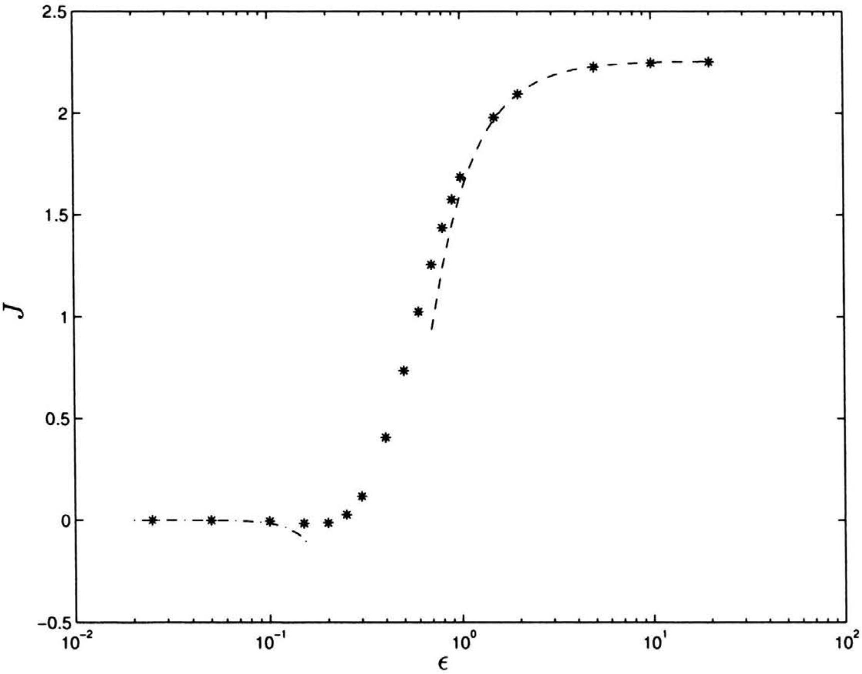

FIGURE 3.2. Normalized migration velocity on a sphere translating in a shear flow, Eq. (3.10): (*) calculation points of [26]; (−·) expansion for small ϵ; (−−) expansion for large ϵ.

in Fig. 3.2. The values of J become quite small for $\epsilon < 0.2$: then there is no lift and Oseen's case is recovered. Note that the expansion for $\epsilon \ll 1$ (dash-dotted curve in Fig. 3.2) is no more valid for $\epsilon > 0.1$.

3.9. Conclusions

The Saffman lift force is often quoted in applications, but is should be emphasized that his result is valid only for $Re \ll \sqrt{Re_\kappa} \ll 1$, which is often forgotten. Under the more general condition $Re \sim \sqrt{Re_\kappa} \ll 1$, Mac Laughlin's result (Sec. 3.8.4) should be used. The sphere is always freely rotating in these calculations. The next order terms, partly appearing in Sec. 3.3.3, have not been fully calculated. Various extensions of Saffman's result appear in Sec. 3.8, and in Chapter 5.

Chapter 4

Regular perturbation solutions for a sphere and walls

In problems considered in this Chapter, the distance l from the sphere centre to walls (see Fig. 4.1) is much smaller than the Saffman distance $a/\sqrt{Re_\kappa}$ and Oseen distance a/Re for which, as explained in Chapter 3, Stokes expansion is no more valid. Cox & Brenner [19] showed that the presence of walls then makes the perturbation problem regular. Although their demonstration is not straightforward, it may be realized intuitively from the figure that the Saffman and Oseen regions occupy only a small portion of the distant field as compared with the walls, so that the main part of the flow field is directed by the boundary conditions in the Stokes region.

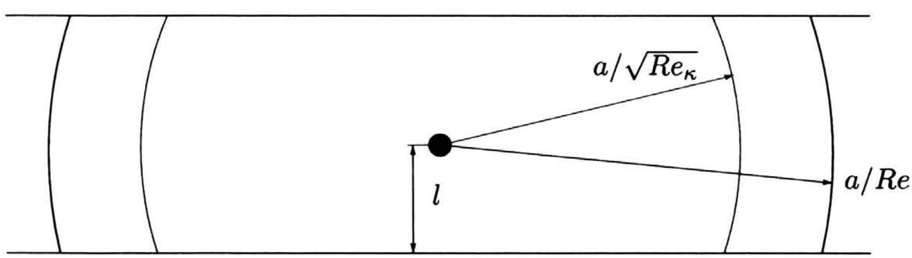

FIGURE 4.1.

4.1. Method of solution for a neutrally buoyant spherical particle

The first authors who applied the formal theory of [19] were Ho & Leal [20] who calculated the inertial migration velocity of a neutrally buoyant freely rotating sphere in a two-dimensional shear flow and in the Poiseuille flow. The presentation below concentrates on the Poiseuille flow.

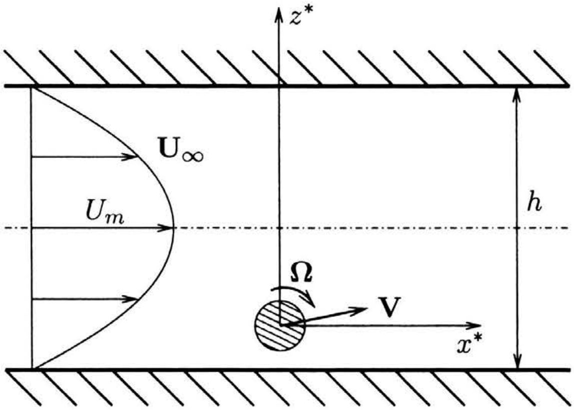

FIGURE 4.2.

Let $\mathbf{U}_\infty$ be the Poiseuille flow velocity. For a neutrally buoyant sphere, the appropriate characteristic velocity is based on the shear rate. But since the local shear rate varies across the flow field, it is easier to build a characteristic velocity based on a global shear rate, that is U_m/h, where U_m is the maximum velocity of the Poiseuille flow and h is the distance between walls. Let $V_c^* = U_m a/h$ be this characteristic velocity. The pertinent Reynolds number is based on a and V_c^*, thus based on the global shear rate:

$$Re_p = \frac{U_m a^2}{\nu h}.$$

This Reynolds number is assumed to be small compared with unity. Normalizing then lengths by a and velocities by V_c^*, we construct dimensionless particle translational and rotational velocities denoted as $\mathbf{v}_p$ and $\boldsymbol{\omega}_p$. These unknown velocities are expanded for small Re_p:

$$\mathbf{v}_p = \mathbf{v}_{p0} + Re_p\,\mathbf{v}_{p1}, \qquad \boldsymbol{\omega}_p = \boldsymbol{\omega}_{p0} + Re_p\,\boldsymbol{\omega}_{p1}.$$

From Bretherton's argument (Sec. 1.2), it is anticipated that $\mathbf{v}_{p0}$ is along the x^* axis. We also construct a dimensionless unperturbed flow velocity denoted as $\mathbf{u}_\infty$. The dimensionless unknown perturbed flow velocity in a frame attached to the sphere centre is written as $\mathbf{u} = \mathbf{u}_\infty - \mathbf{v}_{p0} + \mathbf{v}$, where $\mathbf{v}$ denotes the unknown perturbation velocity.

Since the problem is regular, it is sufficient to use the Stokes equations at orders 0 and 1. The straightforward Stokes expansion consists, as before, in expanding for small Re_p while keeping length scales of the order of the sphere radius. The expansions for the fluid velocity and pressure are written as:

$$\mathbf{v} = \mathbf{v}_0 + Re_p\,\mathbf{v}_1, \qquad p = p_0 + Re_p\,p_1.$$

The Navier Stokes and boundary conditions then become at order 0:

$$\begin{aligned}
\boldsymbol{\nabla}\cdot\mathbf{v}_0 &= 0,\\
\nabla^2\mathbf{v}_0 - \boldsymbol{\nabla}p_0 &= 0,\\
r = 1 &: \mathbf{v}_0 = -\mathbf{u}_\infty + \mathbf{v}_{p0} + \boldsymbol{\omega}_{p0}\times\mathbf{r},\\
\text{On walls} &: \mathbf{v}_0 = 0,\\
r\to\infty &: \mathbf{v}_0 \to 0.
\end{aligned}$$

There are various ways to solve this order 0 Stokes flow problem. In [20], the solution is found by the method of reflexions, assuming that the ratio of the sphere radius to the distance to the nearest wall is small compared with the unity, that is: $a/l \ll 1$. It is found that because of walls the Stokes flow velocity decays fast far from the sphere, $|\mathbf{v}_0| \sim 1/r^2$ for $r \gg 1$.

Next, the Navier Stokes and boundary conditions give at order 1:

$$\begin{aligned}
\boldsymbol{\nabla}\cdot\mathbf{v}_1 &= 0,\\
\nabla^2\mathbf{v}_1 - \boldsymbol{\nabla}p_1 &= \mathbf{v}_0\cdot\nabla\mathbf{v}_0 + \mathbf{v}_0\cdot\nabla\mathbf{u}_\infty + (\mathbf{u}_\infty - \mathbf{v}_{p0})\cdot\nabla\mathbf{v}_0,\\
r = 1 &: \mathbf{v}_1 = \mathbf{v}_{p1} + \boldsymbol{\omega}_{p1}\times\mathbf{r},\\
\text{on walls} &: \mathbf{v}_1 = 0,\\
r\to\infty &: \mathbf{v}_1 \to 0.
\end{aligned}$$

Let $\mathbf{f}$ denote the right-hand-side of the momentum equation. An important result from [20] is a theorem of reciprocity giving a relationship between the force and sphere velocity at order 1. That is, there is no need to calculate the full order 1 flow field in order to obtain such a relationship.

4.2. The theorem of reciprocity connecting orders 0 and 1

Consider two different flow fields for the same fluid volume V_f limited by the spherical particle, the wall and a hemisphere of large radius:

- the unknown order 1 Stokes flow with velocity $\mathbf{v}_1$, pressure p_1, stress tensor $\boldsymbol{\sigma}_1$;
- an alternative order 0 Stokes flow with velocity $\mathbf{w}$, pressure q, stress tensor $\mathbf{t}$, for a sphere moving with unit velocity $\mathbf{e}_z$ normal to walls.

The order 1 momentum equation written in terms of the stress tensor $\boldsymbol{\sigma}_1$ is multiplied by $\mathbf{w}$ and the order 0 momentum equation written in terms of the stress tensor $\mathbf{t}$ is multiplied by $\mathbf{v}_1$:

$$(\nabla \cdot \boldsymbol{\sigma}_1 - \mathbf{f}) \cdot \mathbf{w} = 0, \qquad (\nabla \cdot \mathbf{t}) \cdot \mathbf{v}_1 = 0.$$

Combining and integrating over the fluid volume V_f gives:

$$\int_{V_f} [(\nabla \cdot \boldsymbol{\sigma}_1) \cdot \mathbf{w} - (\nabla \cdot \mathbf{t}) \cdot \mathbf{v}_1]\, dV = \int_{V_f} \mathbf{f} \cdot \mathbf{w}\, dV.$$

Using the expressions for the stress tensors and the continuity equations, it can be shown that, with S_f the surface surrounding the fluid:

$$-\int_{S_f} \mathbf{n} \cdot (\boldsymbol{\sigma}_1 \cdot \mathbf{w} - \mathbf{t} \cdot \mathbf{v}_1)\, dS = \int_{V_f} \mathbf{f} \cdot \mathbf{w}\, dV.$$

Here S_f is the surface made of:

- the walls: the fluid velocity vanishes there;
- the sphere: $\mathbf{w} = \mathbf{e}_z$ and $\mathbf{v}_1 = \mathbf{v}_{p1} + \boldsymbol{\omega}_{p1} \times \mathbf{r}$;
- the large hemisphere, the radius $\mathcal{R}$ of which may be taken $\mathcal{R} \to \infty$. All quantities vanish there fast enough for the integral on this hemisphere to vanish.

The unit vector $\mathbf{n}$ on S_f is pointing into the fluid domain V_f. When the volume $V_f \to \infty$, Ho & Leal [20] showed, using their result for $\mathbf{v}_0$, that the integral on this volume $\int_{V_f} \mathbf{f} \cdot \mathbf{w}\, dV$ is convergent. That is, the perturbation problem is regular. We are left with:

$$\int_{S} \mathbf{n} \cdot (\boldsymbol{\sigma}_1 \cdot \mathbf{w} - \mathbf{t} \cdot \mathbf{v}_1)\, dS = -\int_{V_f} \mathbf{f} \cdot \mathbf{w}\, dV.$$

Replacing $\mathbf{w}$ and $\mathbf{v}_1$ by their values on the sphere S and changing the order of terms in the mixed product gives:

$$\left(\int_S \mathbf{n}\cdot\boldsymbol{\sigma}_1\,dS\right)\cdot\mathbf{e}_z - \left(\int_S \mathbf{n}\cdot\mathbf{t}\,dS\right)\cdot\mathbf{v}_{p1} + \left(\int_S \mathbf{r}\times(\mathbf{n}\cdot\mathbf{t})\,dS\right)\cdot\boldsymbol{\omega}_{p1} = -\int_{V_f}\mathbf{f}\cdot\mathbf{w}\,dV.$$

In this equation,

- the first term on the left-hand-side is the unknown lift force at order 1, F_{1z};
- in the second term the integral is the drag force on the sphere due to the flow $(\mathbf{w}, q)$; by symmetry, this force only has a component along z, say T_z (note that it is negative); thus the second term is $-T_z v_{p1z}$;
- the integral in the third term is the torque for the flow $(\mathbf{w}, q)$; this torque vanishes by symmetry.

As a result, the theorem of reciprocity gives:

$$F_{1z} - T_z v_{p1z} = -\int_{V_f}\mathbf{f}\cdot\mathbf{w}\,dV.$$

At this point, we can consider two possibilities:

1. the particle velocity is given, say $\mathbf{v}_p$. Then, $\mathbf{v}_p = \mathbf{v}_{p0}$ and $\mathbf{v}_{p1} = 0$. Thus, the dimensionless lift force is:

$$F_z = -Re_p\int_{V_f}\mathbf{f}\cdot\mathbf{w}\,dV. \qquad (4.1)$$

2. A freely moving sphere; the force is zero and we obtain the migration velocity

$$V_m = Re_p v_{p1z} = \frac{Re_p}{T_z}\int_{V_f}\mathbf{f}\cdot\mathbf{w}\,dV \qquad (4.2)$$

in which $\mathbf{f} = \mathbf{v}_0\cdot\nabla\mathbf{v}_0 + \mathbf{v}_0\cdot\nabla\mathbf{u}_\infty + (\mathbf{u}_\infty - \mathbf{v}_{p0})\cdot\nabla\mathbf{v}_0$; where $\mathbf{v}_0$ is known from order 0 and $\mathbf{w}$ was calculated with the method of reflexions [20].

As expected, the ratio between the lift force and the migration velocity involves the drag force for a sphere moving perpendicularly to the walls, that is $6\pi a\mu$ if terms of the order of a/l are neglected.

4.3. Results for the lift force (or migration velocity) for a neutrally buoyant spherical particle

4.3.1. Results of Ho & Leal (1974) with corrections of Vasseur & Cox (1976)

Results of [20] were corrected in [22] for the cases where the sphere is near any of the two walls (not too close anyway since $a/l \ll 1$). The lift force is written in dimensional form as:

$$F_z^* = 6\pi\rho \left(\frac{U_m}{h}\right)^2 a^4 K_5^P \left(\frac{l}{h}\right) \tag{4.3}$$

where l is the distance of the sphere centre to one of the walls, viz. l/h increases with z and varies from 0 to 1. Here, K_5^P denotes a dimensionless lift coefficient (the reason for using this notation will appear from a classification introduced in Sec. 4.5.3). The variation of the lift coefficient K_5^P with l/h is represented in Fig. 4.3. If $K_5^P\left(\frac{l}{h}\right) > 0$, the particle is pushed towards higher l/h. It is understood that the lift force applies to a particle which

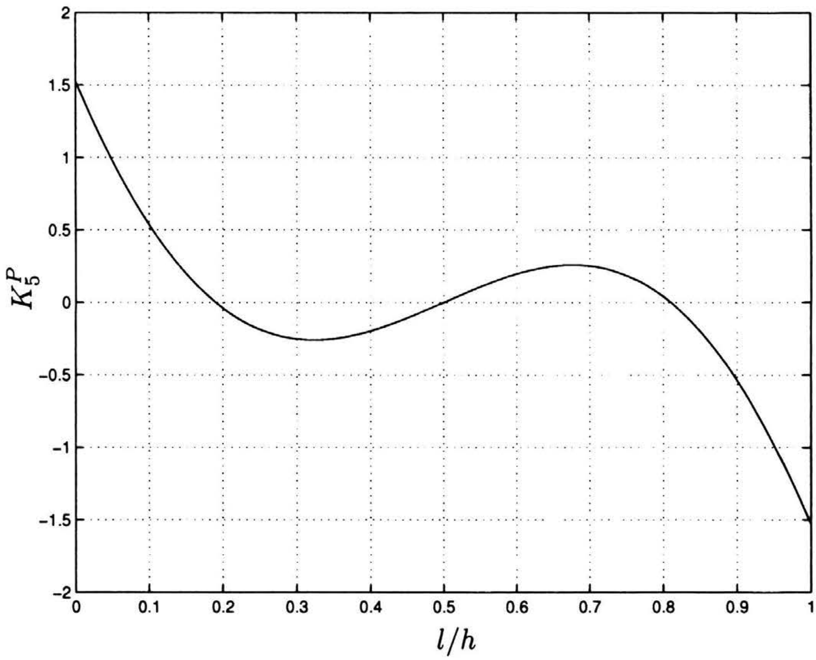

FIGURE 4.3. Lift coefficient on a sphere in Poiseuille flow, as defined in Eq. (4.3) and used in Eq. (4.18). This function is well fitted by the polynomial function (4.17).

is intended of moving in the z direction. To the order considered in the small Reynolds number and ignoring terms of the order of a/l in the friction factor T_z, the migration velocity V_m in the z direction is simply obtained by dividing the lift force by the Stokes friction coefficient $6\pi a\mu$.

In Fig. 4.3, the points where K_5^P vanish give equilibrium positions. From the sign of the lift force, it is realized that there are two stable equilibrium positions. These positions are similar to the ones observed by Segré & Silberberg [9]. Moreover, the lift force in Eq. (4.3) varies with the fluid velocity squared, U_m^2 and like a^4, as also measured in [9]. The theory of [20] was the first one to give a consistent model of the migration observed by Segré & Silberberg [9].

4.3.2. More exact comparison with Segré & Silberberg experiment

The preceding results concern the Poiseuille flow between parallel walls, whereas Segré & Silberberg [9] experiments used the Poiseuille flow in a cylindrical tube. A theory of the lateral migration of a spherical particle in the Poiseuille flow in a circular tube was performed later by Ishii & Hasimoto [23]. Their expansion procedure is similar to that of [20]. The calculation of walls effects is of course different and they used for that purpose the flow due to a Stokeslet in the circular tube, as calculated by Hasimoto [38]. The equilibrium positions are similar to the ones for the flow between parallel walls.

In the calculations of [20] and [23] the Reynolds number based on the canal width and velocity is small compared with unity, whereas this Reynolds number is of the order of $Re_c \sim 20$ in Segré & Silberberg [9] experiments. The case of a larger canal Reynolds number was later considered by Schonberg & Hinch [24] for the Poiseuille flow between parallel walls. Their calculation involves a singular perturbation problem and will be presented later in Chapter 5. To our knowledge, there is no calculation analogous to that of [24] for a circular tube, that is there is no theory matching exactly the conditions of the experiment described in [9].

4.4. Method of solution for a non-neutrally buoyant sphere between two walls

When the sphere is non-neutrally buoyant and has a translational velocity in the same direction as the ambient flow velocity, the migration becomes

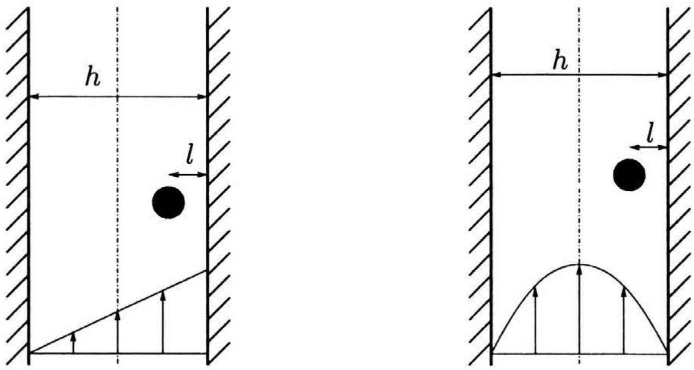

FIGURE 4.4.

different. This problem was studied by Vasseur & Cox [22], Cox & Hsu [39]. Consider then a vertical flow field which may be either a shear flow or the Poiseuille flow, with an embedded non-neutrally buoyant spherical particle.

An expansion in $Re = V a/\nu \ll 1$ is performed and the perturbation problem is regular. Moreover, it is assumed that

$$\frac{a}{h} \ll 1, \quad \text{with: } \frac{a}{l} \ll 1, \quad \frac{a}{(h-l)} \ll 1,$$

viz. they consider a small sphere not close to walls.

To summarize, the solution of [22] goes along the following lines:

- Since $a/h \ll 1$, they consider point particles.
- They use Cox & Brenner [19] result for the migration velocity in terms of integrals on the fluid volume involving the Green function.
- They calculate the Green function for a Stokes flow between parallel walls.
- Their results for the migration velocity in the shear flow and in the Poiseuille flow are obtained for various cases depending on the dimensionless numbers: U_m/V and $U_m/V(a/h)^2$.

The results obtained by Vasseur & Cox [22] for the migration velocity of a non-neutrally buoyant sphere in a fluid at rest, in the shear flow and the 2D Poiseuille flow will be presented in the next Sections.

4.5. Results for the migration velocity of a non-neutrally buoyant sphere

4.5.1. Fluid at rest, or in very slow motion

The first situation, denoted here as "case 1", is that of a sphere moving between parallel walls in a fluid at rest or in very slow motion (let then U_m be its maximum velocity). The result for the migration velocity is:

• **Case 1 :**

$$V_m = \frac{V_x^2 a}{\nu} K_1 \left(\frac{l}{h}\right) \quad \text{if} \quad \frac{U_m}{V} \ll 1, \tag{4.4}$$

where V_x is the x component of $\mathbf{V}$ and $V = |V_x|$. Obviously, the migration velocity is independent of the direction of the sphere motion. The dimensionless lift coefficient K_1 is represented in Fig. 4.5. We may approximate it by a polynomial in

$$\xi = l/h - 1/2$$

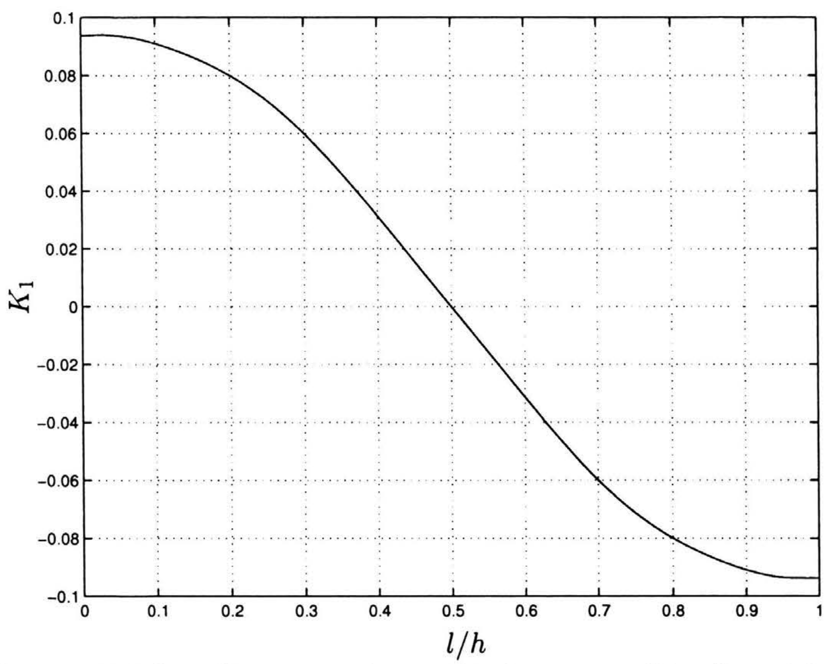

FIGURE 4.5. Lift coefficient on a sphere settling between parallel walls, as defined in Eq. (4.18). This function is well fitted by the polynomial function (4.5).

as follows:

$$K_1\left(\frac{l}{h}\right) = -0.3125\,\xi - 0.0996\,\xi^3 + 14.34\,\xi^5 - 116.3\,\xi^7 + 403.7\,\xi^9 - 518.0\,\xi^{11}. \tag{4.5}$$

4.5.2. Shear flow

Following [19, 22], results are obtained for the following separated cases, denoted here as cases (κ, n), where $n = 2$ to 5:

- **Case** $(\kappa, 2)$ **:**

$$V_m = \frac{V_x^2 a}{\nu}\left[K_1\left(\frac{l}{h}\right) + \frac{U_m}{V_x}K_3^\kappa\left(\frac{l}{h}\right)\right] \quad \text{if} \quad \frac{U_m}{V} = Ord(1). \tag{4.6}$$

- **Case** $(\kappa, 3)$ **:**

$$V_m = \frac{V_x U_m a}{\nu}K_3^\kappa\left(\frac{l}{h}\right) \quad \text{if} \quad \frac{U_m}{V} \gg 1 \quad \text{and} \quad \frac{U_m}{V}\left(\frac{a}{h}\right)^2 \ll 1. \tag{4.7}$$

- **Case** $(\kappa, 4)$ **:**

$$V_m = \frac{V_x U_m a}{\nu}\left[K_3^\kappa\left(\frac{l}{h}\right) + \frac{U_m}{V_x}\left(\frac{a}{h}\right)^2 K_5^\kappa\right] \quad \text{if} \quad \frac{U_m}{V}\left(\frac{a}{h}\right)^2 = Ord(1). \tag{4.8}$$

- **Case** $(\kappa, 5)$ **:**

$$V_m = \frac{U_m^2 a}{\nu}\left(\frac{a}{h}\right)^2 K_5^\kappa \quad \text{if} \quad \frac{U_m}{V}\left(\frac{a}{h}\right)^2 \gg 1. \tag{4.9}$$

Recall that $a/h \ll 1$ in all cases. Note that the orientation of the axis along the walls is irrelevant: indeed, the sign of the migration velocity V_m depends only on the sign of U_m/V_x.

The functions K_3^κ, K_5^κ are represented in Figs. 4.6 and 4.7, respectively, and may be approximated by:

$$K_3^\kappa\left(\frac{l}{h}\right) = -0.0353 + 0.0973\,\xi^2 + 0.2898\,\xi^4 - 0.4363\,\xi^6, \tag{4.10}$$

$$K_5^\kappa\left(\frac{l}{h}\right) = -0.2845\,\xi + 0.4104\,\xi^3 + 0.4165\,\xi^5 - 2.3364\,\xi^7. \tag{4.11}$$

These results for K_5^κ correspond to a freely rotating sphere, the most standard situation. Results for a non-rotating sphere (not shown here) were also found in [22].

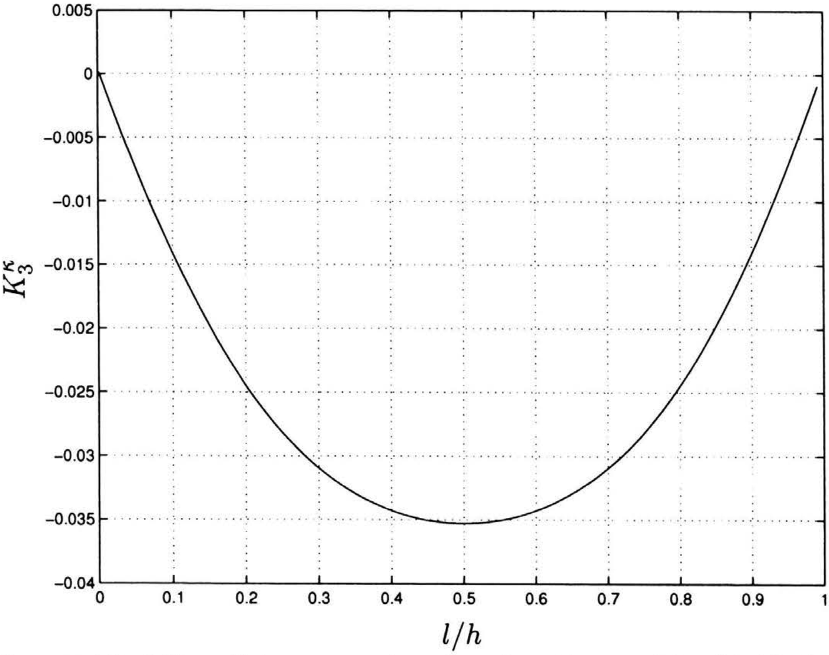

FIGURE 4.6. Lift coefficient on a sphere in a shear flow, as defined in Eq. (4.7). This function is well fitted by the polynomial function (4.10).

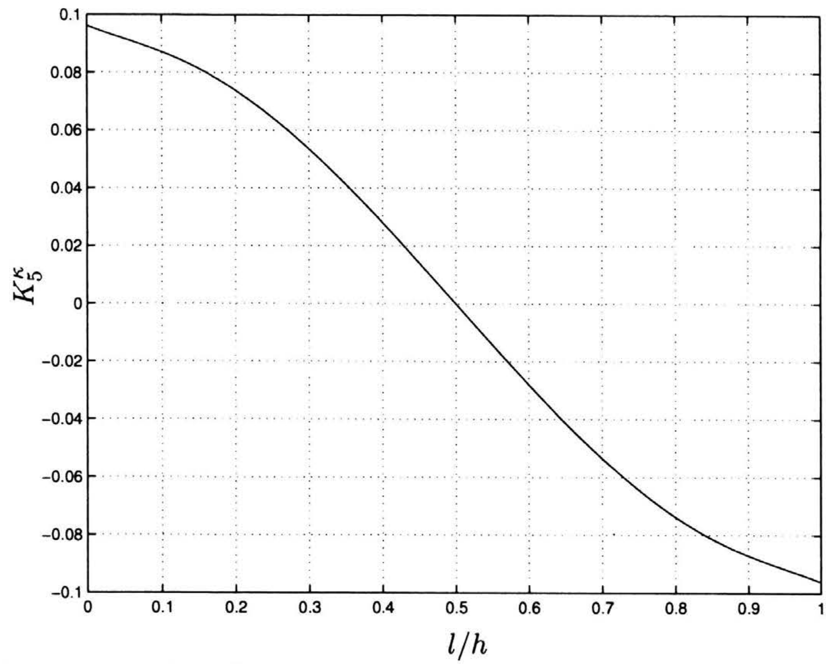

FIGURE 4.7. Lift coefficient on a sphere in a shear flow, as defined in Eq. (4.9). This function is well fitted by the polynomial function (4.11).

4.5.3. 2D Poiseuille flow

Following [19, 22], results are obtained for the following separated cases, denoted here as cases (P,n), where $n = 2$ to 5:

- **Case** $(P,2)$:

$$V_m = \frac{V_x^2 a}{\nu}\left[K_1\left(\frac{l}{h}\right) + \frac{U_m}{V_x}K_3^P\left(\frac{l}{h}\right)\right] \quad \text{if} \quad \frac{U_m}{V} = Ord(1). \qquad (4.12)$$

- **Case** $(P,3)$:

$$V_m = \frac{V_x U_m a}{\nu}K_3^P\left(\frac{l}{h}\right) \quad \text{if} \quad \frac{U_m}{V} \gg 1 \quad \text{and} \quad \frac{U_m}{V}\left(\frac{a}{h}\right)^2 \ll 1. \qquad (4.13)$$

- **Case** $(P,4)$:

$$V_m = \frac{V_x U_m a}{\nu}\left[K_3^P\left(\frac{l}{h}\right) + \frac{U_m}{V_x}\left(\frac{a}{h}\right)^2 K_5^P\left(\frac{l}{h}\right)\right] \qquad (4.14)$$

$$\text{if} \quad \frac{U_m}{V}\left(\frac{a}{h}\right)^2 = Ord(1).$$

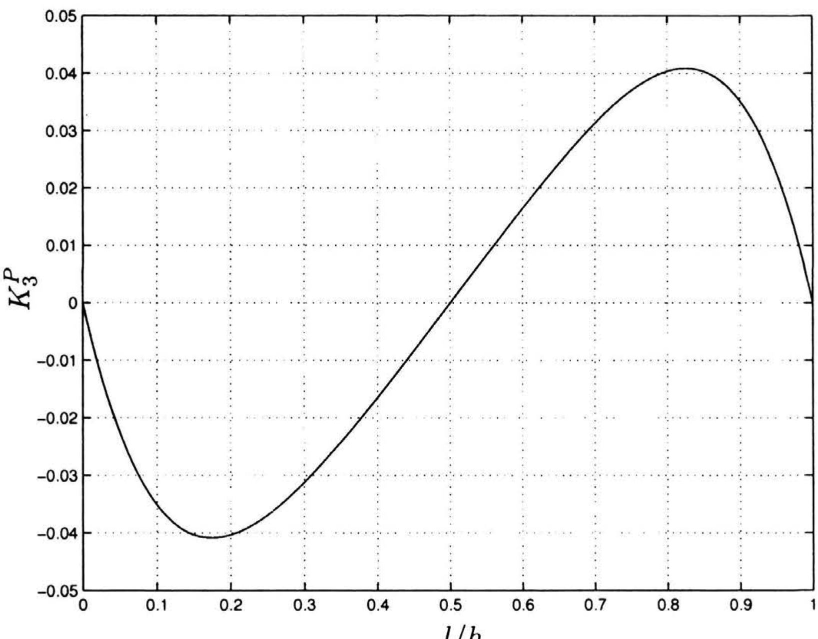

FIGURE 4.8. Lift coefficient on a sphere in Poiseuille flow, as defined in Eq. (4.13). This function is well fitted by the polynomial function (4.16).

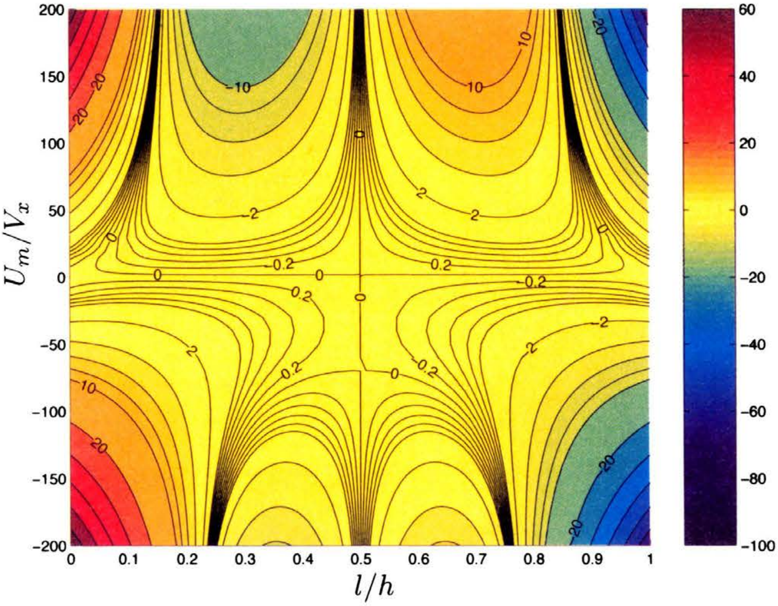

FIGURE 4.9. Contour plot of the normalized migration velocity $V_m/(V_x^2 a/\nu)$ of a non-neutrally buoyant particle in Poiseuille flow, from formula (4.18) for $a/h = 1/30$.

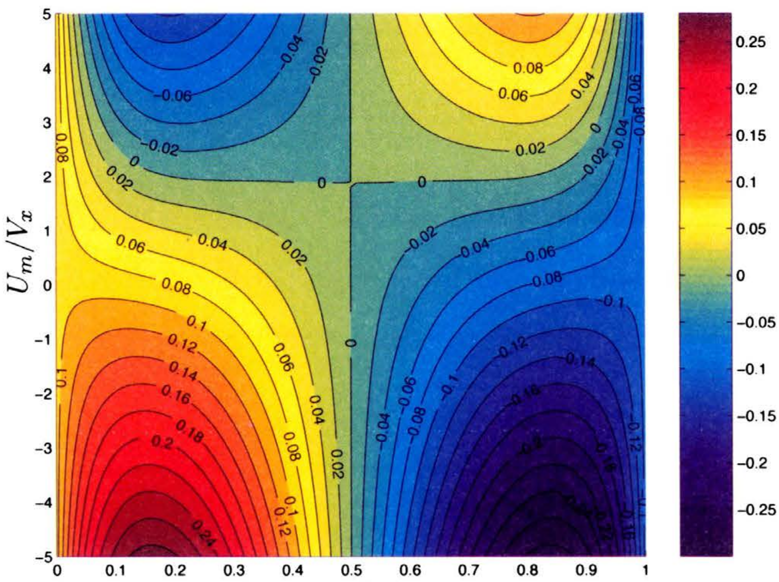

FIGURE 4.10. Contour plot of the normalized migration velocity $V_m/(V_x^2 a/\nu)$ of a non-neutrally buoyant particle in Poiseuille flow, for $a/h = 1/30$; zoom of Fig. 4.9.

• **Case** $(P, 5)$:

$$V_m = \frac{U_m^2 a}{\nu} \left(\frac{a}{h}\right)^2 K_5^P \left(\frac{l}{h}\right) \quad \text{if} \quad \frac{U_m}{V} \left(\frac{a}{h}\right)^2 \gg 1. \tag{4.15}$$

Again, $a/h \ll 1$ in all cases, and the sign of the migration velocity V_m only depends on the sign of U_m/V_x.

The coefficients K_1, K_3^P, K_5^P are represented in Figs. 4.5, 4.8, and 4.3, respectively. K_1 was approximated by a polynomial in (4.5) and K_3^P, K_5^P may be approximated as follows:

$$K_3^P\left(\frac{l}{h}\right) = 1.15\,\xi\,(0.5+\xi)\,(0.5-\xi) \times \left[1 - 1.681\,(0.5+\xi)\,(0.5-\xi)\right], \tag{4.16}$$

$$K_5^P\left(\frac{l}{h}\right) = 19.85\,\xi(0.31-\xi)(0.31+\xi) = 1.91\,\xi - 19.85\,\xi^3. \tag{4.17}$$

These results for K_5^P correspond to a freely rotating sphere, the most standard situation. Results for a non-rotating sphere (not shown here) were also found in [22].

There is no exact solution for intermediate cases and we propose here the following semi-empirical formula which we assume to be valid in all cases:

$$V_m = \frac{V_x^2 a}{\nu}\left[K_1\left(\frac{l}{h}\right) + \frac{U_m}{V_x} K_3^P\left(\frac{l}{h}\right) + \left(\frac{U_m}{V_x}\frac{a}{h}\right)^2 K_5^P\left(\frac{l}{h}\right)\right]. \tag{4.18}$$

The complicated variation of the normalized migration velocity $V_m/(V_x^2 a/\nu)$ with the relative lateral position l/h and ratio U_m/V_x of the maximum Poiseuille flow velocity U_m to the sphere velocity V_x is represented as a contour plot in Figs. 4.9 and 4.10. The example case $a/h = 1/30$ is considered in these figures.

4.6. Equilibrium positions

From the zeros and sign of the migration velocity, various stable equilibrium positions may be derived. These equilibrium positions are sketched in Fig. 4.11. We include for completeness both the shear flow and Poiseuille flow results, for a non-neutrally buoyant sphere as well as for a neutrally buoyant one. Obviously, some cases are symmetric, e.g. a sphere heavier than the

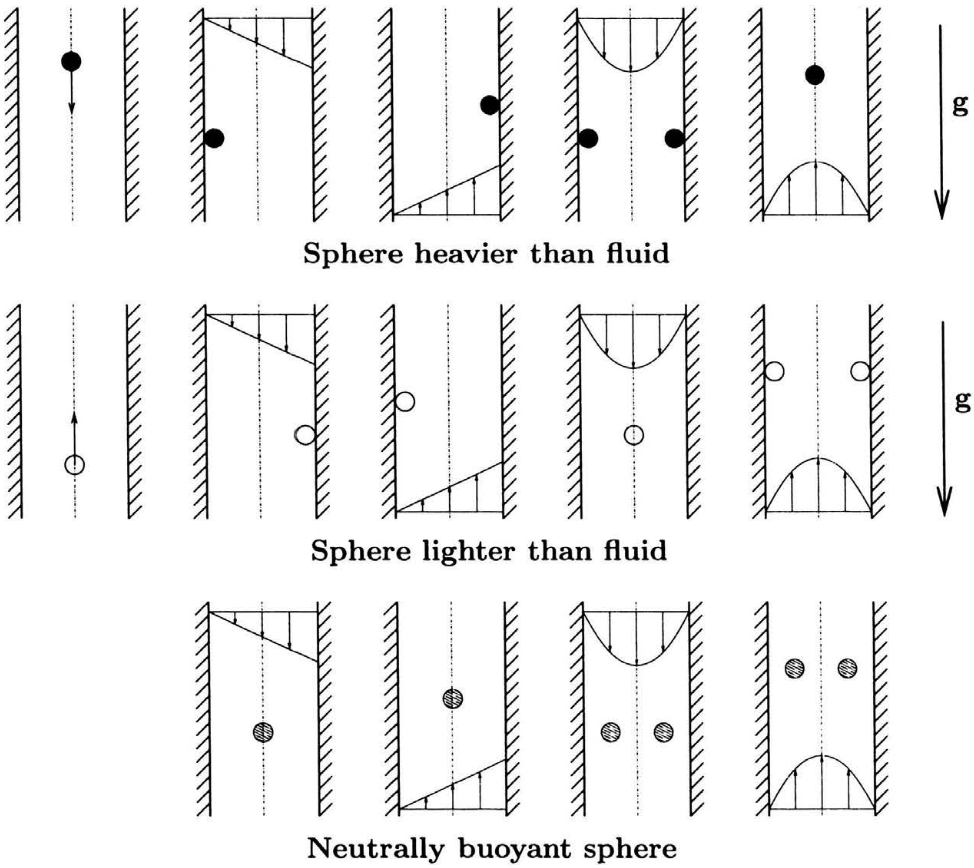

FIGURE 4.11. Schematic representation of the final stable equilibrium positions of a solid spherical particle in a shear flow and in the Poiseuille flow. The circle representing the particle is enlarged for easier reading, but note that this theory assumes that the particle is small compared with the distance between walls. The particle touching the wall is a sketch meaning a final position near the wall (the details of this position are not treated by the present theory).

fluid in a downward flow and a sphere lighter than the fluid in an upward flow. Moreover for a shear flow, attaching the frame of reference to the moving wall gives the alternative equilibrium position. For a neutrally buoyant freely rotating sphere in Poiseuille flow, the stable equilibrium position are at:

$$l/h = 0.19, 0.81\,.$$

Actually, for $U_m/V > 0$, the behaviour is more complicated than sketched in Fig. 4.11. Moreover, for a nearly neutrally buoyant sphere in Poiseuille flow, the stable equilibrium positions are very sensitive to the ratio of densities of the particle and fluid.

Considering the Poiseuille flow, it is observed in Fig. 4.9 that the migration velocity is zero in a large portion of the canal when U_m/V is small compared with 50, but the zoomed Fig. 4.10 shows that this happens for $U_m/V \simeq 2$. Then for $U_m/V > 2$, there are two equilibrium positions, for $l/h \sim 0.1$ to 0.15 and for $l/h \sim 0.85$ to 0.9. For $-70 < U_m/V < 2$ (the approximated lower bound depending on a/l) there is a central equilibrium position. At $U_m/V \simeq -70$ there is a bifurcation and for $U_m/V < -70$ there are again two stable equilibrium positions but at about mid-distance between the canal centreline and the walls. For $|U_m/V| \to \infty$, the Ho & Leal equilibrium positions should be recovered, but it is seen that even a small non-buoyancy may have an important influence.

These various equilibrium positions have not been fully exploited in separation techniques and there is obviously a vast field of applications.

4.7. Lift on a sphere in a shear flow near a wall or in contact with a wall

4.7.1. Method of solution

When a sphere is near a wall, the preceding solutions based on the method of reflexions fail. More precise results have to be used to calculate the hydrodynamic interactions between the sphere and the wall. There are methods using special coordinates to solve such Stokes flow problems: the method of bipolar coordinates (when the sphere is separated from the wall) and the method of tangent sphere coordinates (when the sphere is in contact with the wall). These methods in combination with the theorem of reciprocity of Sec. 4.2 make it possible to calculate the lift force on a sphere near a wall or touching a wall.

The problem of a sphere in a shear flow near a wall was solved in this way by Cherukat & McLaughlin [28]. They used the results calculated in bipolar coordinates by Lin, Lee & Sather [40]. The notation is shown in Fig. 4.12.

This is a regular perturbation problem. The lift force is again from the theorem of reciprocity (4.1) given by:

$$F_z = -Re_p \int_{V_f} \mathbf{f} \cdot \mathbf{w} \, dV$$

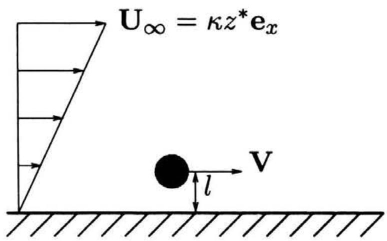

FIGURE 4.12.

where

$$\mathbf{f} = \mathbf{v}_0 \cdot \nabla \mathbf{v}_0 + \mathbf{v}_0 \cdot \nabla \mathbf{u}_\infty + (\mathbf{u}_\infty - \mathbf{v}_{p0}) \cdot \nabla \mathbf{v}_0$$

and V_f denotes the entire fluid volume. The calculation of the integral has to be performed numerically and the sign of F_z is a priori not obvious.

The problem of the sphere in contact with the wall was solved by Leighton & Acrivos [41] for a fixed sphere and by Krishnan & Leighton [42] for a moving sphere. These authors used the solution for the order 0 Stokes flow calculated in tangent sphere coordinates by O'Neill [43].

4.7.2. Results for the lift force on a sphere near a wall

Results of the integration show that, if the sphere is lagging the ambient shear flow, the lift force is pointing away from the wall, towards the direction of higher ambient flow velocity. Numerical values are shown in Fig. 4.13 for the dimensional lift force F_z^* normalized by $a\mu Re_s V_s$, where $V_s = V_x - \kappa l$ is a "slip" velocity (V_x being the x component of $\mathbf{V}$ and κl being the x component of $\mathbf{U}_\infty$ taken at the sphere centre) and $Re_s = V_s a/\nu$ is the Reynolds number based on this velocity. This slip velocity may be due to several reasons: first, there may be an external force moving the sphere along the wall, e.g. the gravity force; then, even a neutrally buoyant sphere does not move at the same velocity as the fluid near a wall, because of hydrodynamic interactions [7, 8]. Cox & Hsu's [39] solution of the singular perturbation problem for sphere far from a wall is shown for comparison in Fig. 4.13. As for the sphere close to the wall, note that the solution calculated in [28] cannot be applied for small gaps, $l/a - 1 < 0.1$. We connected this solution to that for a sphere touching a wall [42] by a spline for practical use. But this approximate curve should not hide the fact that a precise determination of the lift force is lacking for small gaps.

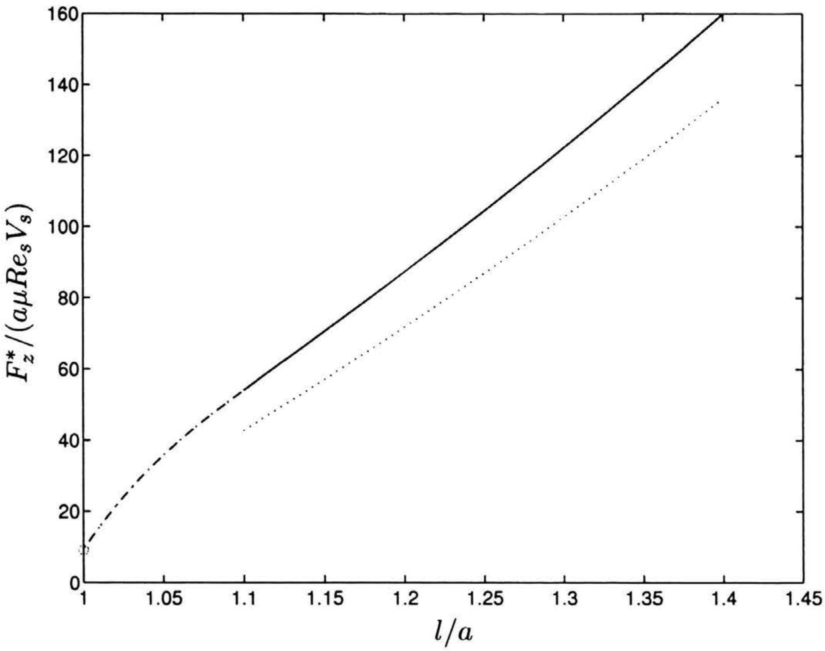

FIGURE 4.13. Results for the normalized lift force on a sphere near a wall: (-) Cherukat & Mc Laughlin [28]; (o) Krishnan & Leighton [42]; (- · -) spline joining both solutions; (· · ·) Cox & Hsu's [39] singular perturbation problem for a sphere far from a wall.

4.7.3. How to lift a particle sitting on a wall?

Leighton & Acrivos [41] result for the lift force exerted on a sphere at rest on a wall is, in dimensional form:

$$F_z^* = 9.22\,\mu\,\kappa\,a^2\,Re_\kappa = 9.22\,\rho\kappa^2 a^4.$$

Consider, e.g., a small solid particle sitting on a wall. Is it possible to entrain this particle by blowing air so that there a lift force pushing the particle away from the wall? As an example, a boundary layer in air at 10 m/s after 1 m has a thickness of the order of a millimetre and the shear rate is then of the order of $10^4 s^{-1}$. Consider for instance a ratio of particle to gas density of $\rho_p/\rho_g = 10^3$ and a particle radius of $a = 100\,\mu$m. Then we calculate that the lift force if 2.2 times the weight of the particle. That is, the particle is entrained. Note, however, that such a shear rate is large and usually for such high velocities, there are other effects connected with turbulent vortices entering the viscous sublayer.

On the other hand, for liquids the lift forces are much more efficient, being proportional to the fluid density ρ. There are various applications: in separation techniques, etc.

4.8. Conclusions

The Segré & Siberberg experiment motivated the elaborated singular perturbation problems solved by Rubinow & Keller (Chapter 2) and Saffman (Chapter 3), but the proper mechanism was eventually obtained from a regular perturbation problem solved by Ho & Leal (Sec. 4.1). Nevertheless the singular perturbation problems presented in the preceding Chapters were useful for the purpose of modelling the experiment, since they were later extended to model situations in which the canal Reynolds number is not small, thereby dropping Ho & Leal assumption; this is the topic of Chapter 5.

Apart from the case of neutrally buoyant particles which were used in the Segré & Siberberg experiment, various interesting situations arise when the particles are non-neutrally buoyant. Then, the migration velocity may vary in a non trivial way with the flow parameters. These results may have various applications in separation techniques and elsewhere.

Chapter 5

Singular perturbation solutions for a sphere and walls

In this Chapter, walls are now in the Saffman or Oseen region. A sketch of the various length scales is presented in Fig. 5.1. The perturbation problems for low Reynolds number are then singular. Appropriate equations in stretched quantities should apply in the Saffman or Oseen region. Boundary conditions on walls should then be applied to the solution of these equations.

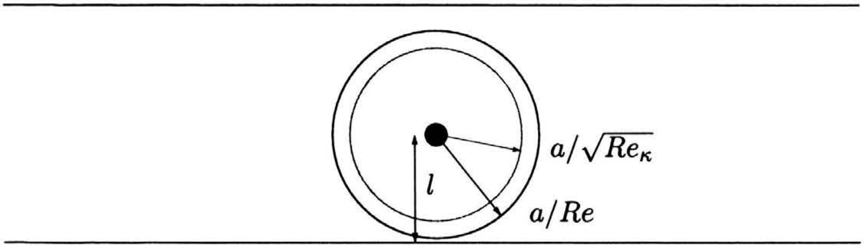

FIGURE 5.1.

5.1. A non-neutrally buoyant sphere between walls in a fluid at rest

5.1.1. Problem and assumptions

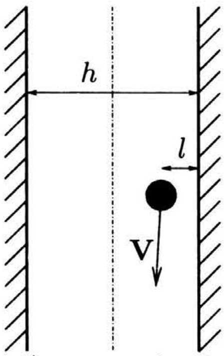

Vasseur & Cox [44] considered the problem of a non-neutrally buoyant spherical particle moving due to gravity in a fluid at rest between vertical parallel walls. The relevant Reynolds number is based on the particle velocity $\mathbf{V}$ and radius a; this number is assumed to be small compared with unity:

$$Re = \frac{Va}{\nu} \ll 1.$$

An expansion in Re is performed under additional assumptions:

$$a/h \ll 1, \qquad \text{with:} \quad a/l \ll 1, \quad a/(h-l) \ll 1,$$

that is they consider a small sphere not close to walls. On the other hand, the Reynolds number based on the particle velocity and distance between the particle and the nearest wall, Vl/ν, may be of the order of unity. This is the main difference as compared with all theories presented in the preceding Chapters.

5.1.2. Oseen equation and boundary conditions

The problem is singular and Oseen equations have to be constructed like in Chapter 2. The matching with the sphere which appears as a point in the Oseen region is performed by introducing a point force or Stokeslet as the Dirac delta function, like in Saffman's approach, Chapter 3:

$$\begin{aligned} \frac{\partial \mathbf{U}_1}{\partial X} &= -\boldsymbol{\nabla} P_1 + \nabla^2 \mathbf{U}_1 - 6\pi \mathbf{e}_x \delta(\mathbf{R}), \\ \boldsymbol{\nabla} \cdot \mathbf{U}_1 &= 0, \\ \text{on walls} &: \quad \mathbf{U}_1 = 0. \end{aligned}$$

The difference as compared with the Saffman problem is that now there is a boundary condition on the walls to be applied to the solution of the equation. For this reason, instead of using a 3 dimensional Fourier transform to solve the equation, a 2 dimensional Fourier transform is used. That is, Z is kept so as to apply the boundary conditions on the walls on which Z is prescribed:

$$\hat{\mathbf{U}}_1(k_1, k_2, Z) = \frac{1}{4\pi^2} \int_{-\infty}^{\infty} \int_{-\infty}^{\infty} \mathbf{U}_1(X, Y, Z) e^{-i(k_1 X + k_2 Y)} \, dX \, dY. \tag{5.1}$$

Applying this Fourier transform to the Oseen like equation leads, after some manipulation, to coupled equations for the Fourier transform of the velocity along Z, $\hat{W}_1$ and for the Fourier transform of the pressure, $\hat{P}_1$. Note that after applying the 2 dimensional Fourier transform to the Oseen like equation, the transform of the three dimensional delta Dirac function gives a remaining $\delta(Z)$. To account for that term, the equation is solved using appropriate jump conditions for the pressure, velocity and its derivatives.

5.1.3. Matching and migration velocity

The part $\mathbf{U}_{S1}$ of $\mathbf{U}_1$ obtained from the point singularity matches with the Stokeslet in Stokes flow (it was made for that purpose). Matching the remaining (regular) part of $\mathbf{U}_1$ gives a uniform flow at infinity for the order 1 Stokes flow (like in the Saffman case, Chapter 3). This is the migration velocity:

$$\begin{aligned} \lim_{R \to 0} (\mathbf{U}_1 - \mathbf{U}_{S1}) &= \lim_{R \to 0} \int (\hat{\mathbf{U}}_1 - \hat{\mathbf{U}}_{S1}) e^{i(k_1 X + k_2 Y)} \, dk_1 \, dk_2 \\ &= \int (\hat{\mathbf{U}}_1 - \hat{\mathbf{U}}_{S1}) \, dk_1 \, dk_2. \end{aligned} \tag{5.2}$$

5.1.4. Results for the migration velocity of a sphere near one wall

Vasseur & Cox [44] recovered the result of [39] for the migration velocity of a sphere settling close to a vertical wall, which was obtained as the solution of a regular perturbation problem when the wall is in the Stokes region:

$$\frac{V_m}{V Re} = \frac{3}{32}.$$

Moreover, their result provides the following expansion for small Vl/ν:

$$\frac{V_m}{V Re} = \frac{3}{32} \left[1 - \frac{11}{32} \left(\frac{Vl}{\nu} \right)^2 + \ldots \right]. \tag{5.3}$$

They also obtained an expansion for large Vl/ν (obviously not too large so that the flow field is still laminar), that is for large distances l from the wall:

$$\frac{V_m}{V Re} = \frac{3}{8}\left[\left(\frac{\nu}{Vl}\right)^2 + 2.21901\left(\frac{\nu}{Vl}\right)^{5/2} + \dots\right]. \tag{5.4}$$

Results for intermediate values of the Reynolds number Vl/ν, that is for intermediate distances l from the wall, are shown in Fig. 5.2.

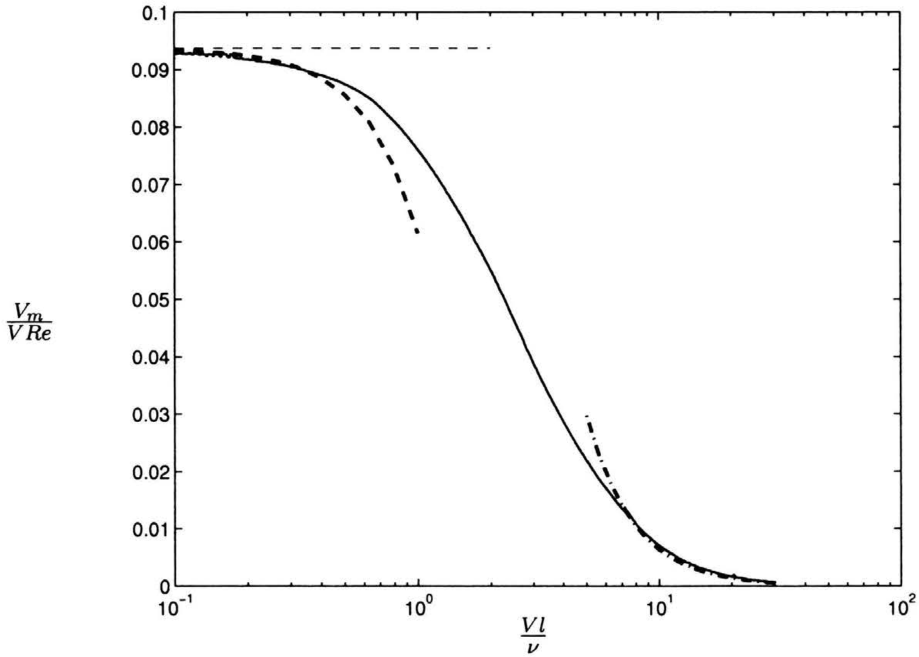

FIGURE 5.2. Values of the normalized migration velocity $V_m/(V Re)$ versus Vl/ν for a sphere settling along one wall; solid line: calculation of [44]; thin horizontal dotted straight line: asymptotic value 3/32; dotted line: formula (5.3); dash-dotted line: formula (5.4).

5.1.5. Results for the migration velocity of a sphere moving between two walls

Here again, Vasseur & Cox [44] recovered the result of [39] for a sphere near one of the walls. Results for two walls effects are shown in Fig. 5.3. It is found that the sphere migrates towards the symmetry plane.

that is

$$\lambda = l/\sqrt{\nu/\kappa}.$$

The most general case considered here is when λ is of the order of unity.

5.2.2. Equation in Saffman region

Including the point force for matching we write:

$$\begin{aligned}\left(\frac{Re}{\sqrt{Re_\kappa}} + \tilde{Z}\right)\frac{\partial \tilde{\mathbf{U}}_1}{\partial \tilde{X}} + \tilde{W}_1 \mathbf{e}_x &= -\tilde{\boldsymbol{\nabla}}\tilde{P}_1 + \tilde{\nabla}^2\tilde{\mathbf{U}}_1 - 6\pi\mathbf{e}_x\delta(\tilde{\mathbf{R}}), \\ \tilde{\boldsymbol{\nabla}}\cdot\tilde{\mathbf{U}}_1 &= 0.\end{aligned}$$

All terms are included like in equation (3.7a) treated by McLaughlin [26] . However, here a condition applies on the wall:

$$\tilde{Z} = 0: \quad \tilde{\mathbf{U}}_1 = 0.$$

The solution of this system uses 2-D Fourier transform (on $\tilde{X}, \tilde{Y}$) like in (5.1). The migration velocity is also found by the same procedure, see Eq. (5.2).

5.2.3. Results for the migration velocity of a sphere in a shear flow near a wall

Results for the reduced migration velocity

$$\frac{V_m}{V_s'(Re_\kappa)^{1/2}}$$

where $V_s' = -V_s$, are presented in term of $1/\epsilon$, the ratio of the Saffman distance to the Oseen distance and of $1/\lambda$, the ratio of the Saffman distance to the distance to the wall as a three-dimensional surface in Fig. 5.4 and as a contour plot in Fig. 5.5.

From these figures we conclude that:

- For $1/\epsilon = 1/\lambda = 0$, the Saffman result:

$$\frac{V_m}{V_s'(Re_\kappa)^{1/2}} = 0.343$$

  is recovered (since without wall V_s' can be identified with V').
- For $1/\lambda = 0$ and any ϵ, the quantity plotted here being $3/(2\pi^2)J$, results for J from Eq. (3.10) may be used.

that is

$$\lambda = l/\sqrt{\nu/\kappa}.$$

The most general case considered here is when λ is of the order of unity.

5.2.2. Equation in Saffman region

Including the point force for matching we write:

$$\left(\frac{Re}{\sqrt{Re_\kappa}} + \tilde{Z}\right)\frac{\partial\tilde{\mathbf{U}}_1}{\partial\tilde{X}} + \tilde{W}_1\mathbf{e}_x = -\tilde{\boldsymbol{\nabla}}\tilde{P}_1 + \tilde{\nabla}^2\tilde{\mathbf{U}}_1 - 6\pi\mathbf{e}_x\delta(\tilde{\mathbf{R}}),$$

$$\tilde{\boldsymbol{\nabla}}\cdot\tilde{\mathbf{U}}_1 = 0.$$

All terms are included like in equation (3.7a) treated by McLaughlin [26] . However, here a condition applies on the wall:

$$\tilde{Z} = 0 : \quad \tilde{\mathbf{U}}_1 = 0.$$

The solution of this system uses 2-D Fourier transform (on $\tilde{X}, \tilde{Y}$) like in (5.1). The migration velocity is also found by the same procedure, see Eq. (5.2).

5.2.3. Results for the migration velocity of a sphere in a shear flow near a wall

Results for the reduced migration velocity

$$\frac{V_m}{V_s'(Re_\kappa)^{1/2}}$$

where $V_s' = -V_s$, are presented in term of $1/\epsilon$, the ratio of the Saffman distance to the Oseen distance and of $1/\lambda$, the ratio of the Saffman distance to the distance to the wall as a three-dimensional surface in Fig. 5.4 and as a contour plot in Fig. 5.5.

From these figures we conclude that:

- For $1/\epsilon = 1/\lambda = 0$, the Saffman result:

$$\frac{V_m}{V_s'(Re_\kappa)^{1/2}} = 0.343$$

  is recovered (since without wall V_s' can be identified with V').
- For $1/\lambda = 0$ and any ϵ, the quantity plotted here being $3/(2\pi^2)J$, results for J from Eq. (3.10) may be used.

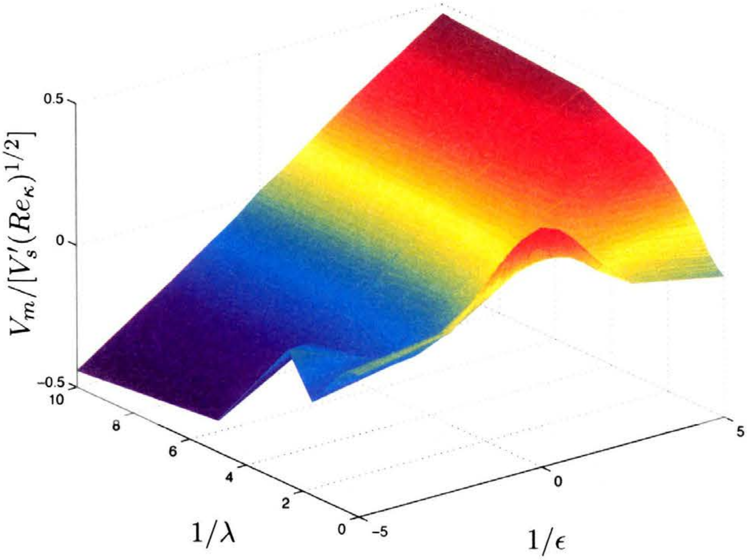

FIGURE 5.4. Normalized migration velocity $V_m/[V_s'(Re_\kappa)^{1/2}]$ of a sphere moving in a shear flow along a wall versus the ratio of the Saffman distance to the Oseen distance, $1/\epsilon$, and the ratio of the Saffman distance to the distance to the wall, $1/\lambda$. Plotted from the results displayed in the tables of [27].

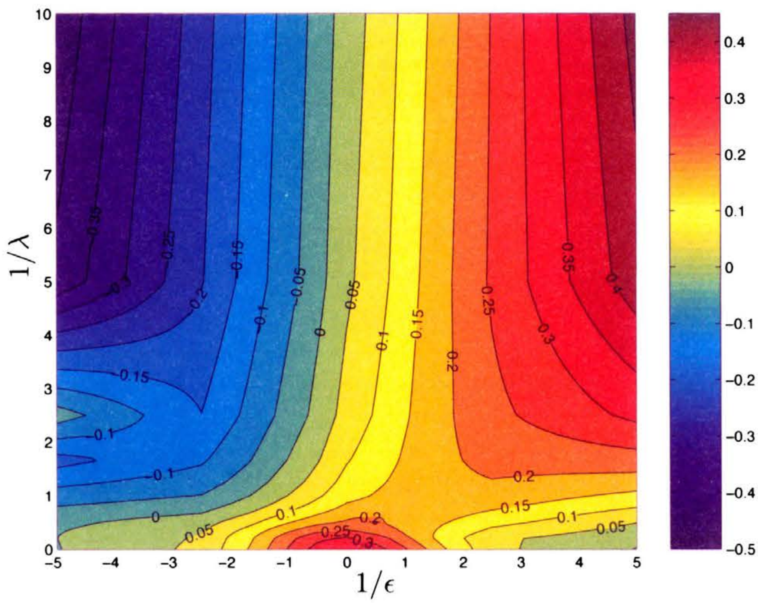

FIGURE 5.5. Contour plot of the reduced migration velocity $V_m/[V_s'(Re_\kappa)^{1/2}]$ of a sphere moving in a shear flow along a wall versus the ratio of the Saffman distance to the Oseen distance, $1/\epsilon$, and the ratio of the Saffman distance to the distance to the wall, $1/\lambda$. Plotted from the results of [27], using a 200×200 mesh and a linear interpolation between the calculation points displayed in the tables of [27].

- For $\lambda \ll 1$, Cox & Hsu [39] derived an expansion which may be written as:
$$\frac{V_m}{V_s'(Re_\kappa)^{1/2}} = \frac{3}{32}\epsilon^{-1} + \frac{11}{64}\lambda.$$
This expansion is recovered here; indeed, it is clear from Fig. 5.4 that for large $1/\lambda$, the surface becomes tangent to a plane.
- $\epsilon < 0$ means here that $V_s < 0$, that is the sphere velocity is smaller than the unperturbed shear flow velocity; note that for given $V_m/[V_s'(Re_\kappa)^{1/2}]$, the migration velocity V_m changes sign with V_s.
- For $\epsilon \ll 1$, shear flow effects are small and the results of Sec. 5.1 should be used.

5.3. A neutrally buoyant sphere in 2D Poiseuille flow

5.3.1. Problem and assumptions

Schonberg & Hinch [24] reconsidered the modelling of the Segré & Silberberg experiment, taking into account the fact that the Reynolds number for the canal should not be small.

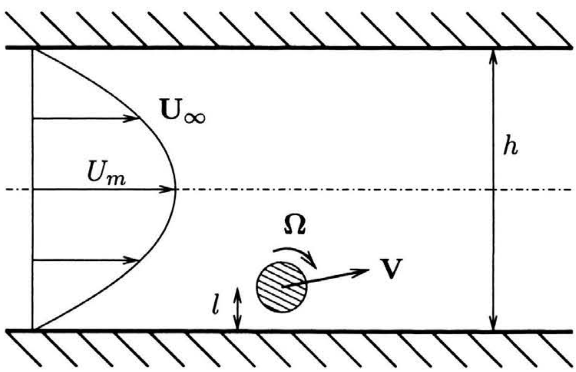

The sphere being centered at the distance l from the wall, the local shear rate at the position of the sphere centre is:

$$\kappa = \frac{\gamma U_m}{h}, \quad \text{where} \quad \gamma = 4 - 8\frac{l}{h}. \tag{5.5}$$

Let z^* denote the coordinate normal to the walls and $z = z^*/a$ the dimensionless one. A normalized local shear flow velocity may be defined as:

$$\frac{\kappa z^* \mathbf{e}_x}{U_m} = \alpha\,\gamma\,z\,\mathbf{e}_x, \quad \text{with} \quad \alpha = \frac{a}{h}.$$

Thus, let the normalized perturbed velocity be $\alpha(\gamma\, z\mathbf{e}_x + \mathbf{u})$.

The Reynolds number based on the local shear rate and the sphere radius is assumed to be small compared with unity. It may be written as:

$$Re_\kappa = \frac{\kappa a^2}{\nu} = \gamma \frac{U_m a^2}{\nu h} = \gamma\, Re_p \ll 1.$$

Note that the normalized local shear rate γ that may be of the order of unity varies across the canal; thus, as already noted in Sec. 4.1, Re_κ is not an appropriate small parameter to use. Instead, Schonberg & Hinch [24] make an expansion in the constant parameter $Re_p \ll 1$. Note that this number may also be written as:

$$Re_p = \alpha^2 \frac{U_m h}{\nu}$$

where $\alpha \ll 1$, and

$$Re_c = \frac{U_m h}{\nu}$$

is the canal Reynolds number, which may be larger than unity (thus appropriate to Segré & Silberberg experiment). Note that Ho & Leal (see Sec. 4.1) also performed an expansion in Re_p, but in Schonberg & Hinch [24] theory the distance between the sphere and the walls is always so large that the walls are in the Saffman region and the perturbation problem is singular.

5.3.2. Order zero Stokes solution

The order zero Stokes solution for the flow field around a freely moving and freely rotating sphere is:

$$\mathbf{u}_0 = -\frac{5}{2}\gamma \frac{xz\mathbf{r}}{r^5} + O\left(\frac{1}{r^4}\right).$$

This is the flow due to the symmetric moment of a Stokeslet, or "Stresslet".

5.3.3. Saffman like equations and solution

In a Saffman region, the variable $\mathbf{r}$ is stretched as: $\tilde{\mathbf{R}} = \sqrt{Re_p}\,\mathbf{r}$. For simplicity of the notation, we use the same tilde $(\tilde{\ })$ notation as in Chapter 3, but care should be taken that the stretched variable defined here is different. On the large scale where $\tilde{R} = |\tilde{\mathbf{R}}|$ is of the order of unity, the Stresslet appears like the flow due to a point singularity, that may be introduced into the momentum equation as the derivative of a delta function. By doing that, the matching condition between the order 0 Stokes equations and the order 1 Saffman like equations is introduced in these equations:

$$\tilde{\boldsymbol{\nabla}} \cdot \tilde{\mathbf{U}}_1 = 0, \qquad (5.6a)$$

$$\left(\gamma \tilde{Z} - 4Re_c^{-1/2} \tilde{Z}^2\right) \frac{\partial \tilde{\mathbf{U}}_1}{\partial \tilde{X}} + \tilde{W}_1 \mathbf{e}_x \left(\gamma - 8Re_c^{-1/2} \tilde{Z}\right) \qquad (5.6b)$$

$$= -\tilde{\boldsymbol{\nabla}} \tilde{P}_1 + \tilde{\nabla}^2 \tilde{\mathbf{U}}_1 - \frac{10\pi}{3} \gamma \left[\frac{\partial}{\partial \tilde{Z}}, 0, \frac{\partial}{\partial \tilde{X}}\right] \delta(\tilde{\mathbf{R}}).$$

Since the walls are in the Saffman region, the following boundary conditions apply:

$$\tilde{Z} = -Re_c^{1/2} \frac{l}{h} \quad \text{and} \quad \tilde{Z} = Re_c^{1/2} \left(1 - \frac{l}{h}\right) \quad : \quad \tilde{\mathbf{U}}_1 = 0.$$

The system is solved by using a 2 dimensional Fourier transform, Eq. (5.1), like was done by Vasseur & Cox. Then coupled equations are obtained for the transformed velocity in the direction normal to walls, $\widehat{\tilde{W}}_1$ and the transformed pressure $\widehat{\tilde{P}}_1$. After transforming the momentum equation, from $\left[\frac{\partial}{\partial \tilde{Z}}, 0, \frac{\partial}{\partial \tilde{X}}\right] \delta(\tilde{\mathbf{R}})$ there is a remaining $\frac{\partial}{\partial \tilde{Z}} \delta(\tilde{Z})$. Thus, the transformed equation is solved using jump conditions for the pressure and for the $\tilde{Z}$-derivative of the velocity.

5.3.4. Matching and migration velocity

The part $\tilde{\mathbf{U}}_{SS}$ of $\tilde{\mathbf{U}}_1$ obtained from the point singularity matches with the Stresslet in Stokes flow. Indeed, the preceding construction of the Saffman like momentum equation (5.6b) was made for that purpose.

The remaining (regular) part of $\tilde{\mathbf{U}}_1$ gives after matching a uniform flow at infinity for the order 1 Stokes flow (like in Saffman [18]). This is the migration velocity:

$$\lim_{\tilde{R} \to 0} (\tilde{\mathbf{U}}_1 - \tilde{\mathbf{U}}_{SS}) = \lim_{\tilde{R} \to 0} \int (\widehat{\tilde{\mathbf{U}}}_1 - \widehat{\tilde{\mathbf{U}}}_{SS}) e^{i(k_1 \tilde{X} + k_2 \tilde{Y})} \, dk_1 \, dk_2$$

$$= \int (\widehat{\tilde{\mathbf{U}}}_1 - \widehat{\tilde{\mathbf{U}}}_{SS}) \, dk_1 \, dk_2.$$

5.3.5. Results for the migration velocity of a neutrally buoyant sphere in a 2D Poiseuille flow

The results for the normalized migration velocity are displayed in Fig. 5.6. The plotted quantity is also the coefficient K_5^P defined in the expression (4.15)

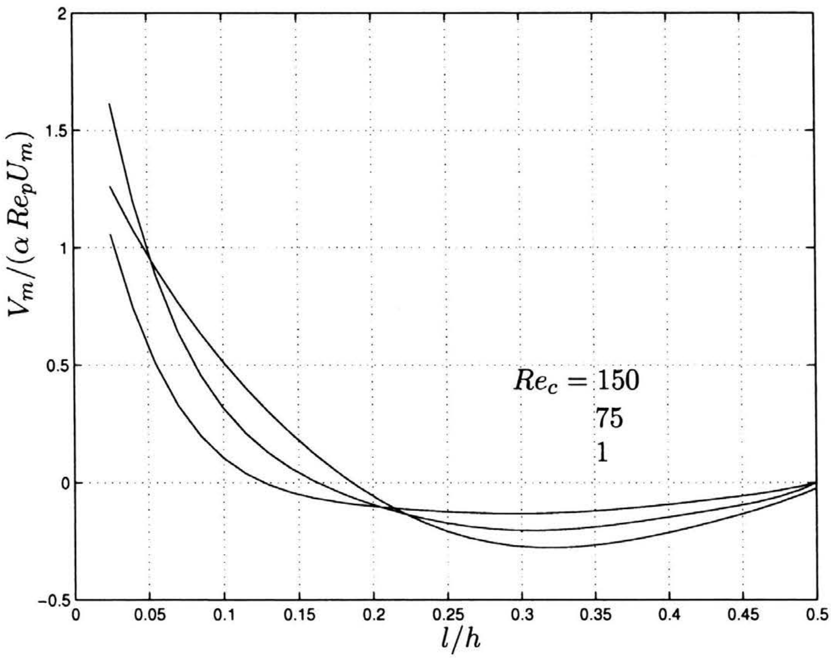

FIGURE 5.6. Results for the normalized migration velocity $V_m/(\alpha\, Re_p\, U_m)$ versus the normalized distance to the wall l/h, for various values of the canal Reynolds number Re_c, after [24].

of V_m (or in (4.3), ignoring terms of the order of a/l in the friction factor T_z), so that the results can be compared to the ones of Fig. 4.3. It is remarkable that for a canal Reynolds number Re_c larger than unity and up to 15, the results obtained in [24] are close to the ones obtained by Vasseur & Cox [22] for $Re_c \ll 1$. For increasing canal Reynolds number, the equilibrium position moves towards the wall, as observed by Segré & Silberberg. However, in their experiment, the particle to wall distance is not large compared with the sphere radius, as assumed in this theory.

5.4. A non-neutrally buoyant sphere in 2D Poiseuille flow

The more general problem of a non-neutrally buoyant sphere in a two-dimensional Poiseuille flow, when the canal Reynolds number is not small, was considered by Hoggs [45] and Asmolov [25]. Here we present the more general result of [25]. In his case, the canal Reynolds number may have values up to 3000. Of course, it is assumed that the flow field stays laminar.

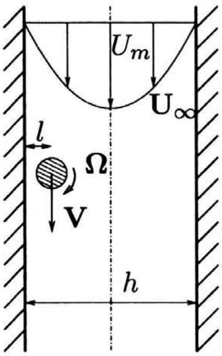

The same local shear rate κ appears like in Eq. (5.5) and it is assumed here that:

$$\sqrt{Re_\kappa} = \sqrt{\frac{\kappa a^2}{\nu}} \sim \sqrt{Re_p} = \sqrt{\frac{U_m a^2}{\nu h}} \sim Re = \frac{Va}{\nu} \ll 1.$$

Asmolov [25] performs two types of expansions: one for small Re_κ, appropriate to a given sphere position, and one for small Re_p like in [24], see Sec. 5.3. We present here the expansion in Re_p. The calculation uses $V_s' = -V_s$, where $V_s = V_x - U_\infty(l/h)$ is the slip velocity, and the normalized velocity $v = \frac{V_s'}{U_m}\sqrt{Re_c}$. Note that for $V_s' > 0$ the particle is lagging the ambient flow field, whereas for $V_s' < 0$, it is ahead of it.

5.4.1. Saffman type equation

Again here, the stretched variable is : $\tilde{\mathbf{R}} = Re_p^{1/2}\mathbf{r}$. The term of the order of $Re_p^{1/2}$ in the expansion satisfies a Saffman like equation:

$$\begin{aligned}
\tilde{\nabla}^2\tilde{\mathbf{U}}_1 - \tilde{\boldsymbol{\nabla}}\tilde{P}_1 - u_\infty\frac{\partial\tilde{\mathbf{U}}_1}{\partial\tilde{X}} - \frac{du_\infty}{d\tilde{Z}}\tilde{W}_1\mathbf{e}_x &= \frac{6\pi v}{Re_c^{1/2}}\mathbf{e}_x\delta(\tilde{\mathbf{R}}),\\
\tilde{\boldsymbol{\nabla}}\cdot\tilde{\mathbf{U}}_1 &= 0,\\
\tilde{\mathbf{U}}_1 = 0 \quad \text{on walls} \quad &: \quad \tilde{Z} = -Re_c^{1/2}\frac{l}{h},\\
&\quad\;\; \tilde{Z} = Re_c^{1/2}\left(1-\frac{l}{h}\right),\\
\tilde{\mathbf{U}}_1 \to 0 \quad \text{as} \quad &: \quad \tilde{X}\to\infty.
\end{aligned}$$

Here, $\tilde{W}_1$ denotes the $\tilde{Z}$ component of $\tilde{\mathbf{U}}_1$ and

$$u_\infty = v + \gamma\tilde{Z} - 4\tilde{Z}^2/Re_c^{1/2}$$

is the flow field far from sphere, in the frame of sphere centre. The equation contains a delta function since the sphere is non-neutrally buoyant and the sphere then appears as a point force in the Saffman region, like in Saffman's original calculation.

5.4.2. Equation for the Fourier transformed velocity normal to walls

The system is solved using again a 2D Fourier transform in $(\tilde{X}, \tilde{Y})$, Eq. (5.1). Combining then the transformed equations, it is shown that the Fourier transform $\widehat{\tilde{W}}_1$ of $\tilde{W}_1$ satisfies:

$$\left(\widehat{\tilde{\Delta}}^2 - ik_1 u_\infty \widehat{\tilde{\Delta}} - 8\frac{ik_1}{Re_c^{1/2}}\right)\widehat{\tilde{W}}_1 = -\frac{3}{2\pi} ik_1 \frac{v}{Re_c^{1/2}} \frac{d\delta(\tilde{Z})}{d\tilde{Z}},$$

$$\widehat{\tilde{W}}_1 = \frac{d\widehat{\tilde{W}}_1}{d\tilde{Z}} = 0 \quad \text{on walls,}$$

where $\widehat{\tilde{\Delta}} = \frac{d^2}{d\tilde{Z}^2} - k_1^2 - k_2^2$ is the Fourier transform of the Laplacian in stretched coordinates. There are numerical difficulties to integrate for $Re_c > 100$ since linearly independent solutions then become of different orders of magnitude. The technique used in [25] then consists in constructing a new set of independent solutions by an orthonormalization procedure.

5.4.3. Results for the migration velocity or the lift force on a non-neutrally buoyant sphere in 2D Poiseuille flow

The order 1 dimensionless migration velocity is obtained as in the preceding theories from matching with the regular part of the Saffman flow, that is subtracting out the Stokeslet part:

$$\frac{V_m}{Re_p^{1/2} U_m} = \lim_{R \to 0} (\tilde{W}_1 - \tilde{W}_S).$$

Asmolov normalizes the migration velocity by the slip velocity:

$$\frac{\frac{V_m}{Re_p^{1/2} U_m}}{\frac{V_s'}{U_m}} = \frac{V_m}{Re_p^{1/2} V_s'}$$

and represents the normalized lift force:

$$6\pi \frac{V_m}{Re_p^{1/2} V_s'}$$

versus l/h for various values of Re_c. Values for a non-neutrally buoyant sphere, for $v = 8, -8$, are displayed in Fig. 5.7. It is observed that for $v = 8$

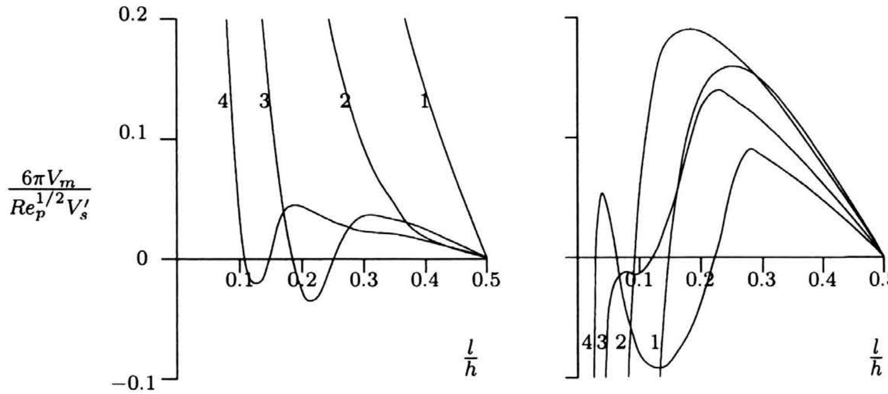

FIGURE 5.7. Values of the normalized lift force $6\pi V_m/[Re_p^{1/2}V_s']$ on a non-neutrally buoyant particle versus the dimensionless distance to one wall, l/h, for $Re_c = 100, 300, 1000, 3000$ (curves 1 to 4), for $v = 8$ (left) and $v = -8$ (right). After [25].

there may be either 1 (curves 1, 2) or 3 (curves 3,4) equilibrium positions; whereas for $v = -8$ there may be either 2 (curves 1, 2, 3) or 4 (curve 4) equilibrium positions.

5.4.4. Equilibrium positions of a neutrally buoyant sphere in 2D Poiseuille flow

Extending the results of [24], Asmolov [25] obtains more values for the migration velocity of a neutrally buoyant sphere. His results, expressed as a normalized lift force

$$\frac{F_z^*}{\rho(U_m/h)^2a^4}$$

are presented in Fig. 5.8. The represented quantity is also the coefficient K_5^P from the definition (4.3). Stable equilibrium positions are found from the zeros and sign of the lift force. From this figure we conclude that for a higher Reynolds number, the equilibrium position is closer to the wall. However, there is still no satisfactory comparison with Segré & Silberberg experiment for large Re_c. The reasons may be summarized as follows:

- Segré & Silberberg use a cylindrical tube.
- The particle Reynolds number Re is not so small in the experiments

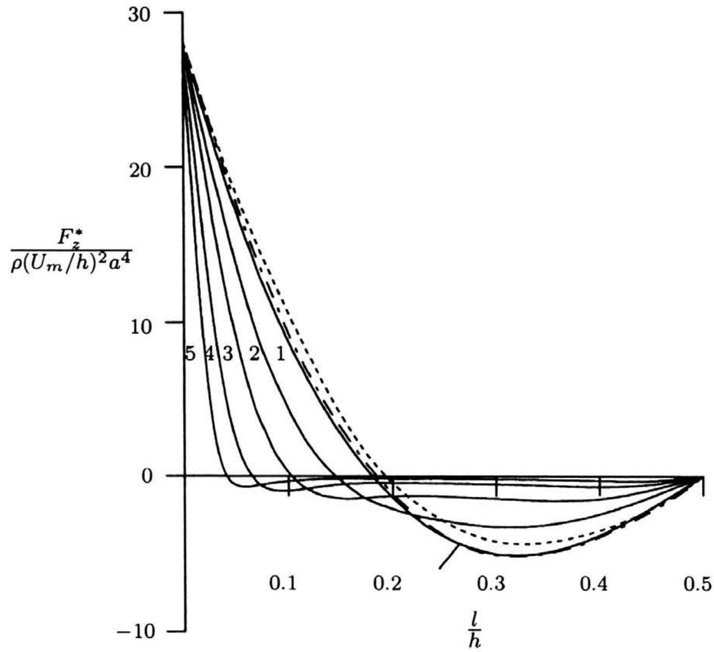

FIGURE 5.8. Values of the normalized lift force $F_z^*/[\rho(U_m/h)^2a^4]$ on a neutrally buoyant particle versus the dimensionless distance to one wall, l/h. Alternatively, this represents $6\pi V_m/[(a/h)Re_pU_m] = 6\pi K_5^P$. Solid lines 1 to 5: for $Re_c = 15, 100, 300, 1000, 3000$ [25]. Dashed-dotted line: for $Re_c = 15$ [24]. Dotted line: for $Re_c \ll 1$ [22].

when Re_c becomes large; indeed the corresponding values are:

Re	Re_c
0.34	116
0.68	232
1.00	346

- The lift force is normalized by a slip velocity; but this quantity is not easily measured.
- Moreover, the slip also depends on the hydrodynamic interactions with walls.

5.5. Conclusions

When walls are in the Oseen or Saffman region, singular perturbation problems arise. Then, even though the Reynolds numbers relative to the particle are small compared with unity, the Reynolds number based on the particle to wall distance or on the canal width is of the order of unity; it may even be larger than unity (but not too large, since the flow is assumed to be laminar).

Various solutions have been presented, for a particle falling in a fluid at rest between two vertical plane walls (Sec. 5.1), for a sphere moving in a shear flow along a wall (Sec. 5.2), for a neutrally buoyant (Sec. 5.3) and non-neutrally buoyant (Sec. 5.4) sphere in two-dimensional Poiseuille flow. Note that the quoted articles contain more results than presented in this Chapter.

Chapter 6

Conclusion

6.1. The quest for the modelling of Segré & Silberberg experiment

The cornerstone experiment of Segré & Silberberg has motivated the solutions of perturbation problems at low Reynolds number for more than 40 years!

The mechanism responsible for particle migration across streamlines in a Poiseuille flow is now clear: it is a combination of fluid inertia appearing in the second order terms of the expansion in small Reynolds number and of wall effects which appear already in the first order (only viscous) terms.

The various perturbation problems have been separated in singular and regular ones (Sec. 1.5.4), depending on how the distance between the sphere centre and the walls compares with the Oseen and Saffman distances.

The singular perturbation problem solved by Rubinow & Keller [21] and presented in Chapter 2 is of interest from the point of view of the calculation technique but following papers are more interesting in term of application of the results.

The pioneer paper of Saffman [18] (presented in detail in Chapter 3) for the singular perturbation problem of a sphere in an infinite shear flow has been a guide for many following theoretical papers. In particular, all following papers apply his matching technique. A large number of papers oriented towards applications quote Saffman force as a synonym of lift force:

care must be taken that the conditions of application prescribed by Saffman are not always taken into account by these papers. In this point of view of applications, results of more recent papers quoted in this review have not been fully exploited.

Cox & Brenner [19] have shown that a number of important problems involving walls are in fact regular. Various problems of this kind have been exposed in Chapter 4. Following this line, Ho & Leal [20] have found the basic mechanism responsible for the migration of neutrally buoyant particles observed in the Segré & Silberberg experiment. Various regular perturbation problems involving non-neutrally buoyant particles and walls have been solved later.

When the Reynolds number based on the length scale of walls is of the order of unity, the perturbation problem is singular and more results for the migration velocity have been found (Cf. Chapter 5), approaching the actual conditions of the Segré & Silberberg experiment. These results may also be of interest in separation techniques; e.g. results by McLaughlin (Sec. 5.2), Asmolov (Sec. 5.4), would deserve various applications.

6.2. What is next?

Yet, Segré & Silberberg experimental results are not fully interpreted! A number of problems remain:

- To our knowledge, the lift force in a cylindrical geometry has only be studied by Hasimoto and coworkers [23, 46] in the case of a low Reynolds number for the pipe flow. But if this Reynolds number is not small compared with unity, the perturbation problem for low particle Reynolds number becomes singular (like for the two-dimensional canal flows presented here); this problem is yet unsolved.
- Effects of a close wall on the motion of a particle are important in particular for the application to separation techniques. More precise estimates of the lift force are needed in the near wall region because this is the region particles are departing from in the FFF separation technique.
- Unsteady fluid flow effects may combine with fluid inertia when the particle-wall geometry varies with time. This is true in particular when the particle is in the near wall region. In this case, in the frame of ref-

erence of the particle centre the flow field is not steady. Then unsteady effects have to be calculated explicitly.

- Various problems concern the interactions between particles, which have not been presented here. Some results concern two spheres and a wall in a fluid at rest [44]. It is clear that more configurations have to be solved.
- In particular, the effect of lift due to fluid inertia has to be compared with the "shear-induced migration" [47], also called "hydrodynamic diffusion" later, that is due to viscous interactions between spheres. Indeed, both effects may occur together, e.g. in separation techniques [14, 48].
- The effect of fluid inertia on hydrodynamic interactions between non spherical particles could be considered as well.

The present booklet was limited to solid particles. For deformable particles, the problem is different since they may migrate across streamlines even within the Stokes flow approximation [49].

Appendix A

Singular perturbation problem and the method of matched asymptotic expansions

A simple singular problem will be first presented on an example, Sec. A.1. The van Dyke and Kaplun matching principles will be recalled in Sec. A.2.

A.1. Friedrichs (1942) example

A.1.1. A singular perturbation problem

This example is taken from van Dyke's book [2]. Consider the following differential equation for $f(x)$:

$$\varepsilon \frac{d^2 f(x)}{dx^2} + \frac{df(x)}{dx} = a, \tag{A.1}$$

$$f(0) = 0, \tag{A.2}$$

$$f(1) = 1, \tag{A.3}$$

in which a is a constant and ε is a small parameter: $\varepsilon \ll 1$. If we let $\varepsilon \to 0$, the first term vanishes and we obtain a first order differential equation. Then we cannot apply both boundary conditions at the same time (except in the particular case $a = 1$). This is a singular perturbation problem. Such a problem appears when a differential equation or a partial differential equations changes type. Usually, it is associated with a problem in the application of boundary conditions.

A.1.2. Outer and inner limits

In the present case, let use keep only the boundary condition (A.3) in $x = 1$. Obviously, the region close to 0 should be treated in some particular way. To study this region in more detail, we use an "inner variable" X defined by:

$$x = \varepsilon X, \qquad f(x) = F(X). \tag{A.4}$$

We call the "inner limit" the limit $\varepsilon \to 0$ when keeping $X = Ord(1)$. With this inner limit, $x \to 0$ with ε. Note that the limit $\varepsilon \to 0$ was taken above by keeping implicitly $x = Ord(1)$: this is the "outer limit".

A.1.3. Inner solution

In inner variable, the system (A.1), (A.2), (A.3) becomes:

$$\frac{d^2F(X)}{dX^2} + \frac{dF(X)}{dX} = a\varepsilon, \tag{A.5}$$

$$F(0) = 0, \qquad F(1/\varepsilon) = 1. \tag{A.6}$$

Applying the inner limit, this system becomes:

$$\frac{d^2F(X)}{dX^2} + \frac{dF(X)}{dX} = 0, \tag{A.7}$$

$$F(0) = 0, \tag{A.8}$$

$$F(\infty) = 1. \tag{A.9}$$

At this stage, since we study the region close to $X = 0$, we just keep the boundary condition (A.8) and drop the boundary condition (A.9). The solution of this system, or "inner solution", is:

$$F(X) = C\left(1 - e^{-X}\right) \tag{A.10}$$

where C is a constant.

A.1.4. Outer solution

With the outer limit, and dropping the boundary condition (A.2), the system (A.1), (A.3) becomes:

$$\frac{df(x)}{dx} = a, \tag{A.11}$$

$$f(1) = 1. \tag{A.12}$$

Its solution, that is the "outer solution", is:

$$f(x) = 1 - a + ax. \tag{A.13}$$

A.1.5. Matching

We dropped the condition (A.2) at $x = 0$ for the outer solution and the condition (A.3) at $x = 1$ for the inner solution. Instead, we "match" these two solutions in the following way:

1. with the outer variable x, the inner region $X = Ord(1)$ appears to be at $x = 0$ when $\varepsilon \to 0$;
2. with the inner variable X, the outer region $x = Ord(1)$ appears to be at $X = \infty$ when $\varepsilon \to 0$.

Then, van Dyke matching principle consists in prescribing that the solution should have the same value in these limit regions:

$$f(0) = F(\infty). \tag{A.14}$$

Applying it here, we find the constant: $C = 1 - a$.

A.1.6. Compare the inner and outer solution with exact solution

The interest of Friedrichs example is that the solution of the system (A.1), (A.2), (A.3) can be calculated exactly with the result:

$$f(x) = (1-a)\frac{1-e^{-x/\varepsilon}}{1-e^{-1/\varepsilon}} + ax. \tag{A.15}$$

This solution is plotted in Fig. A.1 together with the outer and inner solutions, in the example case $a = 0.4$. It is observed that the exact solution is close to the outer solution near $x = 1$ and the to the inner solution near $x = 0$. On the other hand, both outer and inner solutions are rather far from the exact one for intermediate values of x.

A.1.7. Composite expansion

For this reason, it is useful to obtain a better approximation to the solution by combining the outer and inner expansions into a "composite expansion". Van Dyke proposes to construct it in the following way:

$$f_{\text{composite}}(x) = f(x) + F(X) - \text{Ct} \tag{A.16}$$

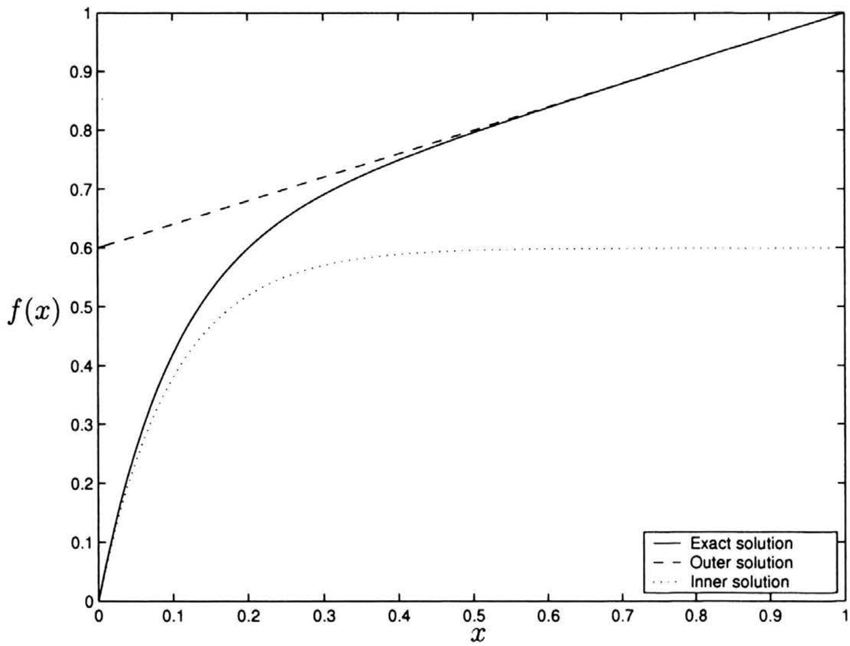

FIGURE A.1. Friedrichs example for the example case $a = 0.4$: exact solution (solid line), outer solution (dashed line) and inner solution (dotted line). The composite expansion is practically superimposed onto the exact solution.

where the constant Ct is the common value obtained by matching

$$\mathrm{Ct} = \lim_{x\to 0} f(x) = \lim_{X\to\infty} F(X).$$

Here, $\mathrm{Ct} = 1 - a$. Values of the composite expansion $f_{\mathrm{composite}}(x)$ are practically superimposed onto the exact solution in Fig. A.1.

A.2. Other more elaborate matching principles

In principle, the outer and inner expansion can be constructed further term by term. At each stage of the construction, a matching has to be applied.

A.2.1. Van Dyke matching principle

The most classical one is due to van Dyke [2]:

m terms inner expansion of the (n terms outer expansion)
$=$ n terms outer expansion of the (m terms inner expansion).

Note that this matching principle assumes a priori that the outer expansion can be expressed in the region where the inner expansion is valid, and vice versa. Obviously, this is not always true.

A.2.2. Kaplun matching principle

The outer region being where $x = Ord(1)$ and the inner region where $x = Ord(\sigma(\varepsilon))$, in which $\sigma(\varepsilon)$ is a function which vanishes with ε, it may happen that both inner and outer expansion are valid simultaneously only in a limited domain of x such that:

$$Ord(\sigma(\varepsilon)) < Ord(x) < Ord(1).$$

Kaplun's [17] matching principle consist in rewriting the outer and inner expansions in an intermediate variable $\tilde{X}$ appropriate to the intermediate domain, expanding again for $\tilde{X} = Ord(1)$ and prescribing that both expansions should then be identical.

Bibliography

1. V. G. Levich, *Physicochemical hydrodynamics*, Prentice Hall, 1962.

2. M. van Dyke, *Perturbation methods in fluid mechanics*, 2nd ed., The Parabolic Press, Stanford, California, 1975.

3. G. G. Stokes, On the effect of the internal friction of fluids on the motion of pendulums, *Trans. Cambridge Phil. Soc.*, Vol. 9, p. 8, 1851.

4. J. Happel and H. Brenner, *Low Reynolds number hydrodynamics*, Dordrecht, Boston, London: Kluwer Academic Publishers, 1991.

5. F. P. Bretherton, The motion of rigid particles in a shear flow at low Reynolds number, *J. Fluid Mech.*, Vol. 14, p. 284, 1962.

6. A. J. Goldman, R. G. Cox, and H. Brenner, Slow viscous motion of a sphere parallel to a plane wall. I. Motion through a quiescent fluid, *Chem. Eng. Sci.*, Vol. 22, pp. 637–651, 1967.

7. A. J. Goldman, R. G. Cox, and H. Brenner, Slow viscous motion of a sphere parallel to a plane wall. II. Couette flow. *Chem. Eng. Sci.*, Vol. 22, pp. 653–660, 1967.

8. M. Chaoui and F. Feuillebois, Creeping flow around a sphere in a shear flow close to a wall, *Quart. J. Mech. Applied Math.*, Vol. 56, No. 3, pp. 381–410, 2003.

9. G. Segré and A. Silberberg, Radial particle displacements in Poiseuille flow of suspensions, *Nature*, Vol. 189, No. 4760, pp. 209–210, 1961.

10. G. Segré and A. Silberberg, Behaviour of macroscopic rigid spheres in Poiseuille flow. 1. Determination of local concentration by statistical analysis of particle passages through crossed light beams, *J. Fluid Mech.*, Vol. 14, pp. 115–135, 1962.

11. G. Segré and A. Silberberg, Behaviour of macroscopic rigid spheres in Poiseuille flow. 2. Experimental results and interpretation, *J. Fluid Mech.*, Vol. 14, pp. 136–157, 1962.

12. H. M. Barkla and L. J. Auchterlonie, The Magnus or Robins effect on rotating spheres, *J. Fluid Mech.*, Vol. 47, pp. 437–447, 1971.

13. H. Brenner, Hydrodynamic resistance of particles at small Reynolds numbers, in: *Advances in Chemical Engineering*, T. B. Drew, Ed., Academic Press, 1966, Vol. 6, pp. 287–431.

14. M. Martin, Theory of field-flow fractionation, in: *Advances in Chromatography*, P.R.Brown and E.Grushka, Eds., Marcel Dekker, New York, 1998, pp. 1–138.

15. A. N. Whitehead, Second approximation to viscous fluid motion, *Quart. J. Pure Applied Maths.*, Vol. 23, pp. 143–152, 1889.

16. C. W. Oseen, Über den Gültigkeitsbereich der Stokesschen Widerstandsformel, *Arkiv for Matematik, Astronomi och Fysik*, Vol. 9, No. 16, pp. 1–15, 1914.

17. S. Kaplun, Fluid mechanics and singular perturbations, in: *A collection of papers by Saul Kaplun*, P. A. Lagerstrom, L. N. Howard, and C.-S. Liu, Eds., Academic Press, 1967.

18. P. G. Saffman, The lift on a small sphere in a slow shear flow, *J. Fluid Mech.*, Vol. 22, pp. 385–400, 1965, corrigendum: *J. Fluid Mech.*, Vol. 31, p. 624, 1968.

19. R. G. Cox and H. Brenner, The lateral migration of solid particles in Poiseuille flow, *Chem. Eng. Sci.*, Vol. 23, pp. 147–173, 1968.

20. B. P. Ho and L. G. Leal, Inertial migration of rigid spheres in two-dimensional unidirectional flows, *J. Fluid Mech.*, Vol. 65, pp. 365–400, 1974.

21. S. I. Rubinow and J. B. Keller, The transverse force on a spinning sphere moving in a viscous fluid, *J. Fluid Mech.*, Vol. 11, pp. 447–459, 1961.

22. P. Vasseur and R. G. Cox, The lateral migration of a spherical particle in two-dimensional shear flows, *J. Fluid Mech.*, Vol. 78, pp. 385–413, 1976.

23. K. Ishii and H. Hasimoto, Lateral migration of a spherical particle in flows in a circular tube, *J. Phys. Soc. Japan*, Vol. 48, No. 6, pp. 2144–2155, 1980.

24. J. A. Schonberg and E. J. Hinch, Inertial migration of a sphere in Poiseuille flow, *J. Fluid Mech.*, Vol. 203, pp. 517–524, 1989.

25. E. S. Asmolov, The inertial lift on a spherical particle in a plane Poiseuille flow at large channel Reynolds number, *J. Fluid Mech.*, Vol. 381, pp. 63–87, 1999.

26. J. McLaughlin, Inertial migration of a small particle in a linear shear flows. *J. Fluid Mech.*, Vol. 224, pp. 261–274, 1991.

27. J. McLaughlin, The lift on a small sphere in wall-bounded linear shear flows, *J. Fluid Mech.*, Vol. 246, pp. 249–265, 1993.

28. P. Cherukat and J. McLaughlin, The inertial lift on a rigid sphere in a linear shear flow field near a flat wall, *J. Fluid Mech.*, Vol. 263, pp. 1–18, 1994, corrigendum: *J. Fluid Mech.*, Vol. 285, p. 407, 1995.

29. H. Lamb, *Hydrodynamics*, Cambridge University Press, 1932.

30. W. Chester, D. R. Breach, and I. Proudman, On the flow past a sphere at low Reynolds number, *J. Fluid Mech.*, Vol. 37, pp. 751–760, 1969.

31. E. Y. Harper and I.-D. Chang, Maximum dissipation resulting from lift in a slow viscous shear flow, *J. Fluid Mech.*, Vol. 33, pp. 209–225, 1968.

32. K. Miyazaki, D. Bedeaux, and J. Bonet Avalos, Drag on a sphere in slow shear flow, *J. Fluid Mech.*, Vol. 296, pp. 373–390, 1995.

33. C. J. Lin, J. H. Peery, and S. W. R., Simple shear flow round a rigid sphere: inertial effects and suspension rheology, *J. Fluid Mech.*, Vol. 44, pp. 1–17, 1970.

34. H. Herron, H. Davis, and P. Bretherton, On the sedimentation of a sphere in a centrifuge, *J. Fluid Mech.*, Vol. 68, pp. 209–234, 1975.

35. S. Childress, The slow motion of a sphere in a rotating viscous fluid, *J. Fluid Mech.*, Vol. 20, pp. 305–314, 1964.

36. D. A. Drew, The force on a small sphere in slow viscous flow, *J. Fluid Mech.*, Vol. 88, pp. 393–400, 1978.

37. F. Feuillebois, Some theoretical results for the motion of solid spherical particles in a viscous fluid, in: *Multiphase Science and Technology*, G. F. Hewitt, J. M. Delhaye, and N. Zuber, Eds., New York: Hemisphere Publishing Co, 1989, pp. 583–789.

38. H. Hasimoto, Slow motion of a small sphere in a cylindrical domain, *J. Phys. Soc. Japan*, Vol. 41, No. 6, pp. 2143–2144, 1976.

39. R. G. Cox and S. K. Hsu, The lateral migration of solid particles in a laminar flow near a plane, *Int. J. Multiph. Flow*, Vol. 3, pp. 201–222, 1977.

40. C. J. Lin, K. J. Lee, and S. N. F., Slow motion of two spheres in a shear field, *J. Fluid Mech.*, Vol. 43, pp. 35–47, 1970.

41. D. Leighton and A. Acrivos, The lift on a small sphere touching a plane in the presence of a simple shear flow, *J. Appl. Math. Phys. (ZAMP)*, Vol. 36, No. 1, pp. 174–178, 1985.

42. G. Krishnan and D. J. Leighton, Inertial lift on a moving sphere in contact with a plane wall in a shear flow, *Phys. Fluids*, Vol. 7, No. 11, pp. 2538–2545, 1995.

43. M. E. O'NEILL, A sphere in contact with a plane wall in a slow linear shear flow, *Chem. Eng. Sci.*, Vol. 23, pp. 1293–1298, 1968.

44. P. VASSEUR and R. G. COX, The lateral migration of spherical particles sedimenting in a stagnant bounded fluid, *J. Fluid Mech.*, Vol. 80, pp. 561–591, 1977.

45. A. J. HOGG, The inertial migration of non-neutrally buoyant spherical particles in two-dimensional shear flows, *J. Fluid Mech.*, Vol. 272, pp. 285–318, 1994.

46. M. SHINOHARA and H. HASHIMOTO[1)], The lateral force on a small sphere sedimenting in a viscous fluid bounded by a cylindrical wall, *J. Phys. Soc. Japan*, Vol. 46, No. 1, pp. 320–327, 1979.

47. D. LEIGHTON and A. ACRIVOS, The shear-induced migration of particles in concentrated suspensions, *J. Fluid Mech.*, Vol. 181, pp. 415–439, 1987.

48. M. H. et P. KUROWSKI, Rôle des forces de portance et diffusion hydrodynamique dans les processus de séparation par la technique de SPLITT, *J. Physique IV*, Vol. 11, pp. 76–81, 2001.

49. H. L. GOLDSMITH and S. G. MASON, *The microrheology of dispersions*, F. R. Eirich ed., ser. Rheology, theory and applications, Academic Press, 1966, Vol. 4, pp. 85–250.

[1)] also spelled Hasimoto in other publications